3-OST-7 REGULATES CARDIAC FUNCTION

AND DEVELOPMENT

IN ZEBRAFISH

by

Shiela C. Samson

A dissertation submitted to the faculty of
The University of Utah
in partial fulfillment of the requirements for the degree of

Doctor of Philosophy

Department of Neurobiology and Anatomy

The University of Utah

May 2011

ProQuest LLC
789 East Eisenhower Parkway
P.O. Box 1346
Ann Arbor, MI 48106-1346

The University of Utah Graduate School

STATEMENT OF DISSERTATION APPROVAL

The dissertation of **Shiela C. Samson**

has been approved by the following supervisory committee members:

H. Joseph Yost	, Chair	**03/03/11** Date Approved
Anne Moon	, Member	**03/03/11** Date Approved
Tatjana Piotrowski	, Member	**03/03/11** Date Approved
Jody Rosenblatt	, Member	**03/03/11** Date Approved
Martin Tristani-Firouzi	, Member	**03/03/11** Date Approved

and by **Monica Vetter**, Chair of

the Department of **Neurobiology and Anatomy**

and by Charles A. Wight, Dean of The Graduate School.

ABSTRACT

Heparan sulfate proteoglycans (HSPGs) are biologically relevant molecules composed of core proteins and glycosaminoglycan (GAG) chains. The location of HSPGs, on the cell surface or in the extracellular matrix, and their structural heterogeneity place them at a unique advantage to influence signaling pathways and cell-cell or cell-matrix interactions. Most of the genes that code for the core proteins and the enzymes that build and modify the GAG chains have been identified. One type of modification, 3-O-sulfation, is catalyzed by a family of 3-O-sulfotransferases (3-OSTs) in zebrafish. Gene expression studies suggest they could modulate different steps of zebrafish development, but the specific roles of each 3-OST have not been elucidated. My dissertation focused on the functions a particular 3-OST, 3-OST-7, perform in zebrafish heart development.

To elucidate the functions of 3-OST-7 in zebrafish heart development, I knocked down 3-OST-7 using morpholinos and found that 3-OST-7 controls ventricular contraction. Analysis of the noncontracting ventricle phenotype in 3-OST-7 morphants demonstrated that *tropomyosin4* is required to mediate 3-OST-7 regulation of ventricular contraction, placing 3-OST-7 upstream of a novel pathway that controls coordinated sarcomere assembly.

Further analysis of the 3-OST-7 knockdown model illustrated that 3-OST-7 functions in two distinct pathways that regulate ventricular maturation. First, 3-OST-7 is

necessary for transforming the isometric ventricular cardiomyocytes into their elongated form. Second, 3-OST-7 shares a feedback loop with *bmp4* signaling to regulate contraction. These findings demonstrated the specificity of 3-OST-7 action towards influencing cardiac development.

Moreover, these studies highlighted the strength of the 3-OST-7 knockdown model in teasing apart the relationship between structure and function. I anticipate that further investigation of this model could advance our understanding of the interrelationships between HSPGs and the signaling pathways that orchestrate cardiac formation.

For Daddy and Nanay

TABLE OF CONTENTS

LIST OF FIGURES

ACKNOWLEDGMENTS

I am and will forever be grateful to the scientific community who helped me through this long, sometimes frustrating, but definitely enriching experience of graduate school. Thank you, Joe Yost, for being my mentor, for improving my science, for taking the time to read over my drafts and offer helpful suggestions, and more importantly, for the kindness and patience you've shown me through this learning process. I also thank the rest of my committee: Anne Moon, Tatjana Piotrowski, Jody Rosenblatt, and Martin Tristani-Firouzi for listening to me during my talks and our meetings, for helping me out with my project, and offering me encouragement. My sincere thanks to the wonderful people of the Yost lab, without whom I would have been lost figuring out how to do experiments, how to make sense of my project, how to give a talk, and how to write a dissertation, among other things. Thanks to my collaborators Martin Tristani-Firouzi and Neil Chi, who have offered technical expertise in analyzing aspects of cardiac excitation which have significantly contributed to this project.

Thank you to people in the CZAR and our lab for taking care of our fish; to people in the Core Facilities, who made sure I have the primers I needed, who sent me sequencing results, who helped me with confocal microscopy and sectioning techniques, and who helped produce and analyze the microarray results; without you, a sizeable fraction of my experiments would not have been done. Thank you to people who have helped my project by sharing their antibodies, their plasmids, their fish, and their time;

particularly noteworthy are Priya Choudhry, Renee Bend, and Norman Hu. I am grateful to have been able to interact with people from the Molecular Biology Program, Department of Oncological Sciences, Neurobiology and Anatomy Department, and the Zebrafish Interest Group, who have all been extremely helpful and supportive, lending me technical support, providing feedback on my presentations, and extending their warmth and friendship. A huge thanks goes out to the zebrafish community outside the University of Utah who have been generous of their plasmids and fish.

Thank you to Barbara Saffel, Tami Brunson, Dee DalPonte, Karen Evans, Monica Vetter, Sheryl Scott, and the International Center staff for making sure I stay in good academic and visa status. Thanks to Teresa Upton for scheduling my meetings with Joe and the venues for my committee meetings, ordering reagents for the lab, and for satisfying my late-afternoon chocolate cravings.

Thank you to my mentors at the University of the Philippines, Ameurfina Santos, Windell Rivera, and Lourdes Cruz, who have all inspired me to become a better scientist.

Lastly, but definitely not the least, my heartfelt thanks to my family and friends: to Daddy, Nanay, Carlo, and my aunts in Sydney, you may not have been here in Salt Lake most of the time, but I constantly feel your love and support reaching out to me across the distance; to my friends who I knew before coming here, your emails are a constant source of laughter and emotional sustenance; and to the friends I met here, I have come to regard you as my family away from home.

The authors for Chapter 2 are Shiela C. Samson, Tania Ferrer, Chuanchau J. Jou, Neil C. Chi, Martin Tristani-Firouzi, and H. Joseph Yost. The authors for Chapter 3 are Shiela C. Samson and H. Joseph Yost. Both works are in preparation for publication.

CHAPTER 1

INTRODUCTION

Vertebrate heart development is a complex process that involves precise coordination of patterning events and cell movements in order to generate a fully formed and functional heart. A molecular framework has emerged that elucidates the commitment of exclusive lineages to discrete regions of the heart, and the underlying cellular decisions that direct the three-dimensional events of cardiac formation. Despite these advances in our understanding of heart development, critical questions remain in the field and unknown players remain to be discovered. Answering these questions and identifying these players could lead to significant advances in the ability to repair or regenerate damaged cardiac tissue via stem cell therapy, and in the ability to diagnose and correct devastating human heart malformations.

What is exceptional about the process of cardiac formation is that the heart begins to function while it continues to develop, and in doing so, shapes its own development. This provides a unique and excellent model for studying not only how form affects function, but how function affects form as well. The relationship between form and function of the heart has been of considerable interest, particularly to those studying late-onset or acquired cardiac diseases, such as the cardiomyopathies. Studies in this area have shown that poor myocardial function causes the heart to compensate by remodeling.

This dissertation will examine the relationship between form and function of the heart during its early stages of development. It will also focus on the patterning and formation of the heart's contractile chambers in zebrafish and examine how this occurs in the context of biologically relevant modifications on heparan sulfate proteoglycans. This will hopefully promote a deeper understanding of heart development and a greater appreciation of its stunning intricacies.

Overview of vertebrate heart development

Studies in different model organisms have demonstrated a program of heart development that has been conserved throughout evolution. The cells of the developing heart come from two distinct mesodermal heart fields that arise and segregate from a common origin (Kelly et al., 2001; Cai et al., 2003; Abu-Issa et al., 2004). The well-studied primary heart field (PHF) originates from cells in the anterior lateral plate mesoderm (LPM) (Srivastava, 2006). The cells of the PHF migrate to coalesce along the ventral midline forming a primitive linear heart tube consisting of an inner endocardial layer and an outer myocardial layer, separated by extracellular matrix (Garry and Olson, 2006). The tube then undergoes morphogenetic movements and differential growth that result in rightward looping and chamber formation (Buckingham et al., 2005). The secondary heart field (SHF) originates from the pharyngeal mesoderm located medial to the PHF (Garry and Olson, 2006). Cells from the SHF begin migrating to the midline when the tube is forming and position themselves dorsal to the heart tube (Srivastava, 2006). When the heart tube starts looping to the right, the SHF migrates to the anterior and posterior portions of the tube, contributing primarily to the outflow tract (OFT) and right ventricle (Kelly et al., 2001; Cai et al., 2003; Laugwitz et al., 2005).

In addition to possessing certain features that make zebrafish especially suitable for investigating cardiac formation (Stainier and Fishman, 1994), the early stages of its heart development are highly conserved with a few minor differences. In zebrafish the PHF appears as bilateral sheets similar to those seen in chick, but in contrast to the cardiac crescent formed in mouse (Stalsberg and DeHaan, 1969; Parameswaran and Tam, 1995; Yelon et al., 1999). These bilateral sheets in zebrafish migrate to the midline, where they fuse and form a cardiac cone (Yelon et al., 1999). This cone gradually elongates to form the primitive heart tube. The heart tube transforms into a two-chambered organ between 24 hours postfertilization (hpf) and 48 hpf through the processes of looping, constriction at the atrioventricular canal (AVC), and bulging of the chambers (Auman et al., 2007). The SHF in zebrafish is not as well studied as in chick and mouse, but it has been observed that new, late-differentiating cardiomyocytes are added to the arterial and venous poles of the heart between 24 hpf and 48 hpf (de Pater et al., 2009).

Myocardial development - specification

The term specification refers to the period where patterning and growth of undifferentiated cardiomyocyte precursors occur. In zebrafish, specification begins during gastrulation, as suggested by pharmacological inhibition of the FGF, BMP, and Hedgehog signaling pathways, which have been shown to be important in this early step of cardiac development (Marques et al., 2008; Thomas et al., 2008; Marques and Yelon, 2009). After gastrulation, molecular markers including *nkx2.5*, *tbx5*, *tbx20*, *gata4*, *gata5*, *gata6*, and *hand2* can be used to identify the heart field in the LPM (Evans et al., 2010). As these markers are also expressed in neighboring, noncardiac tissue or only in a subset

of cardiac precursors, it is necessary to use these markers combinatorially to define the location of the heart field (Raffin et al., 2000; Schoenebeck et al., 2007).

The BMP, FGF, and Nodal pathways have been shown to provide key signals that specify the myocardial fate. Zebrafish mutants for members of these pathways such as *bmp2b*/*swirl*, *fgf8*/*ace*, and *oep* have reduced numbers of cardiomyocytes correlated with reduced expression of cardiac lineage markers such as *nkx2.5* (Reifers et al., 2000; Reiter et al., 2001). Likewise, *smoothened* mutants, which exhibit perturbed Hedgehog signaling, also have decreased numbers of myocardial precursors (Thomas et al., 2008). In contrast to these pathways that positively reinforce cardiac specification, pathways involved in endothelial and hematopoietic specification have been shown to restrict it. Fate mapping studies in zebrafish mutants lacking vessel and blood lineages demonstrated that their enlarged hearts and ectopic cardiomyocytes result from transformation of mesodermal regions known to give rise to vessel and blood lineages (Schoenebeck et al., 2007). Together these studies suggest these signals are integrated in the heart field for commitment to the cardiac lineage. How they are integrated remains largely unknown.

Myocardial development - differentiation

Differentiation is defined by the subspecialization of specified myocardial precursors and is accompanied by downregulation of proliferative pathways and upregulation of differentiation pathways. Discussion of this topic is subdivided into a general overview of pathways involved in early stages of differentiation, a look at myofibrillogenesis and generation of the heartbeat, and finally focusing on the

importance of delineating chamber from nonchamber myocardium in the steps of cardiac maturation.

Pathways regulating early stages of differentiation

It has been demonstrated that differentiation is mediated by BMP signaling, the activity of the T-box (Tbx) family of transcription factors, canonical and noncanonical Wnt signaling, and Hedgehog signaling (Evans et al., 2010). In *Xenopus*, expression of a dominant-negative activin-like kinase 3 receptor inhibited expression of differentiation markers (Shi et al., 2000; Walters et al., 2001; Yang et al., 2006). Furthermore, BMP signaling has been shown to be required for maintaining *tbx20* expression in the developing heart (Mandel et al., 2010).

Knockout or knockdown of *tbx20* in different animal models causes a progressive loss of cardiomyocytes, and defects in looping, chamber formation and maturation (Brown et al., 2005; Cai et al., 2005; Singh et al., 2005; Stennard et al., 2005), highlighting its importance in cardiac differentiation. In contrast to *tbx20*, *tbx1* negatively regulates differentiation. Ectopic expression of differentiation genes including *raldh2*, *gata4*, and *tbx5* and a subset of muscle contractile genes occurs in *tbx1*-null mice (Liao et al., 2008).

Similar to the contrasting activity of *tbx20* and *tbx1*, the canonical and non-canonical Wnt signaling pathways appear to have opposing actions on differentiation. Constitutive activation of β-catenin in SHF precursors, where it has been shown to be important in proliferation, inhibits differentiation (Ai et al., 2007; Cohen et al., 2007; Kwon et al., 2007; Qyang et al., 2007). Despite this role of β-catenin in proliferation, it can also activate Wnt11, which signals through the noncanonical pathway and regulates

an important facet of cardiac differentiation, cell polarity (Phillips et al., 2005; Zhou et al., 2007). Hedgehog signaling is another pathway that needs to be downregulated. SHF-specific ablation of the smoothened receptor results in premature differentiation in mouse (Goddeeris et al., 2008).

In summary, these pathways act in concert or in an antagonistic fashion to promote cardiac differentiation. It remains to be explored how these pathways are orchestrated to promote a single fate, that of the mature and functional heart, and to know the identity of the players that direct these activities. Furthermore, most of these studies were done in mouse and it would be interesting to know whether they hold true in zebrafish as well.

Myofibrillogenesis

An important aspect of differentiation is the expression and assembly of proteins directly linked to the function of the heart. For the heart to contract, contractile proteins must be produced and assembled in units called sarcomeres. This process termed myofibrillogenesis gives rise to a sarcomere that is composed of a thick filament system, composed mostly of myosin, and a thin filament system, consisting of actin, troponin, and tropomyosin. This highly organized structure ensures coordinated generation of force by regulating interaction of actin and myosin filaments. Thus, it is without surprise that mutations in many sarcomeric genes are found in human patients with cardiomyopathies (Clark et al., 2002).

Systematic genetic studies of sarcomeric genes in an *in vivo* model are lacking, however there are several models of myofibrillogenesis (Sanger et al., 2005; Boateng and Goldspink, 2008). In the first model, a stress-fiber like structure serves as the framework

for subsequent sarcomere assembly (Dlugosz et al., 1984). The second model proposes that thick and thin filaments are first assembled independently before being joined together to form a myofibril (Schultheiss et al., 1990; Holtzer et al., 1997; Ojima et al., 1999). The third model stresses that myofibrils arise from preexisting myofibrils along the cell membrane (Rhee et al., 1994; Dabiri et al., 1997). These preexisting myofibrils are shorter versions of the mature sarcomere and lengthen only when titin binds them (Du et al., 2003; Du et al., 2008). Unlike these three models, the fourth model proposes that sarcomere assembly is a concurrent event without the need for intermediate structures (Ehler et al., 1999; Ehler et al., 2004). A study in zebrafish using immunohistochemistry to visualize sarcomere proteins supported the first three models, observed at different assembly steps during myobrillogenesis (Huang et al., 2009).

Large-scale mutagenesis screens in zebrafish have yielded several mutations for sarcomere genes that affect contraction including *cardiac troponin T*, *titin*, *atrial myosin heavy chain*, *cardiac myosin light chain 2*, and *tropomyosin 4* (Sehnert et al., 2002; Xu et al., 2002; Berdougo et al., 2003; Rottbauer et al., 2006; Zhao et al., 2008). Some of these studies demonstrated that loss of a sarcomere protein impacts on the stability of other sarcomere proteins and the sarcomere as a whole (Sehnert et al., 2002; Zhao et al., 2008). Together these studies establish the importance of a properly assembled sarcomere for normal heart contraction.

Generation of heartbeat

Generation of the heartbeat can be analyzed in the context of the process of excitation-contraction coupling. This is a physiological process whereby an electrical stimulus (action potential) is converted to a mechanical response (contraction) (Stern,

1992). Electrical stimulus initiates a sequence of events involving the influx and efflux of various ions resulting in an action potential and a depolarized membrane. Ca^{2+} ions which enter the cell during these events positively reinforce the subsequent release of more calcium ions from the sarcoplasmic reticulum (SR) (Bers, 2002). Ca^{2+} then binds the troponin C subunit (TnC) of the cardiac troponin complex (Gordon et al., 2001). This upregulates the interaction between TnC and another troponin subunit, TnI, resulting in reduced interaction between TnI and actin (Tobacman, 1996; Solaro and Rarick, 1998). Once TnI and actin detach from each other, tropomyosin moves over actin uncovering the myosin binding sites (Vibert et al., 1997; Gordon et al., 2001). Myosin binds and pulls actin towards the center of the sarcomere, effectively shortening the sarcomere and generating contraction.

These events highlight the importance not only of the sarcomere in generating the heartbeat, but also the requirement for upstream players that couple excitation and contraction. This includes, but is not limited to, the plasma membrane ion channels that allow influx and efflux of Na^{+}, K^{+}, and Ca^{2+} ions, and the SR membrane calcium channels that mediate release and re-uptake of Ca^{2+} ions.

Another important aspect of a functional heartbeat is for atrial or ventricular cardiomyocytes to undergo coordinated contraction and this occurs by conduction of the electrical signal to adjacent cells. Electrical stimulation is initiated by pacemaker cells in the sinoatrial (SA) node. This stimulation is then communicated to neighboring atrial cardiomyocytes through gap junctions that allow passage of Ca^{2+} ions. Propagation of electrical activation is interrupted at the AV node, allowing the ventricular chamber to fill

while the atrium contracts. The electrical impulse is then conveyed through gap junctions from the AV node to the ventricular cells.

Contraction initiates during the late stages of heart tube formation prior to looping, raising the possibility that all steps subsequent to this may be affected by this mechanical action. Several studies have shown that abnormal heart function and defective cardiac morphogenesis are correlated (Rottbauer et al., 2001; Xu et al., 2002; Berdougo et al., 2003; Huang et al., 2003). However, the intermediate steps and the signaling pathways involved are not well elucidated.

Chamber (working) and nonchamber (nonworking) myocardium

The ability of the myocardial cells to contract in a coordinated and directed manner is a result of patterning in the heart tube that gives rise to specialized regions. These specialized regions can be grouped under the more general categories of chamber myocardium (atrium and ventricle) and nonchamber myocardium (sinus venosus (SV), AV canal and outflow tract). Nonchamber myocardium retains most of the properties of the primitive heart tube, whereas chamber myocardium has undergone more elaborate differentiation to achieve mature form and function. The chamber and nonchamber myocardium are delineated by a code controlled by the Tbx family (Hoogaars et al., 2007). Region-specific expression of *tbx* genes confers regional identity by activation of identity-promoting genes and repression of identity-opposing genes.

Localized expression of *tbx2* at the AV canal confers identity to this region and represses expression of chamber-specific genes including *atrial natriuretic factor* (*anf*), *chisel*, and the gap junction genes *connexin* (*cx*) *40* and *cx43* (Christoffels et al., 2004). Ectopic expression of *tbx2* in chamber myocardium represses chamber-specific genes

(Christoffels et al., 2004). Interaction with Nkx2.5 is required to repress *anf* (Habets et al., 2002). *Tbx3* is co-expressed with *tbx2* at the AV canal and OFT, and is required for OFT alignment, ventricular septation, and repression of chamber-specific genes in the AV canal (Bakker et al., 2008; Mesbah et al., 2008). *Tbx5* is expressed in the atria and left ventricle, and maintains expression of *anf* and *cx40* (Bruneau et al., 2001). *Tbx18* is expressed in SV and in a subset of SA node cells and ensures that these regions develop normally (Wiese et al., 2009). In contrast to the restricted expression of the *tbx* members mentioned thus far, *tbx20* is expressed throughout the developing heart. Despite this expression pattern, it appears to act only in chamber myocardium where it activates expression of chamber-specific genes and represses *tbx2* expression in ventricular myocardium (Cai et al., 2005; Singh et al., 2005; Stennard et al., 2005).

In addition to the transcriptional network controlled by the Tbx family, various signaling pathways have also been demonstrated to regulate patterning of the heart tube. Notably, BMP signaling has been implicated in regulating AV patterning, which requires AV-specific expression of *bmp2* and *bmp4* (Jiao et al., 2003; Ma et al., 2005). *Bmp2* is upstream of *tbx2*, activating its expression in the AVC (Ma et al., 2005; Park et al., 2006). It is not known whether *bmp4* acts similarly. Upstream of *bmp2* and *bmp4* is the Notch signaling pathway, acting through Hey2 proteins (Rutenberg et al., 2006). Mouse mutant for *hey2* have an expanded AV canal expression of *bmp2*. Similarly, zebrafish mutant for *hey2* (gridlock) have ectopic expression of *bmp4* in the ventricle.

In conjunction with the molecular signatures that distinguish chamber from nonchamber myocardium, several structural and conduction differences arise in these two kinds of myocardium. Chamber myocardium, through later processes of differentiation,

develop high gap-junction density, high conduction velocity, and pronounced trabeculation for ventricular myocardium (Rutenberg et al., 2006). In contrast nonchamber myocardium resembles the primitive heart tube with regards to its strong auto-rhythmicity due to poor intercellular coupling. The number and size of gap junctions is small, and Cx40 and Cx43 are rare or undetectable in nonchamber myocardium (Arguello et al., 1988; van Kempen et al., 1991; Fromaget et al., 1992; Gourdie et al., 1992; Gros et al., 1994). Moreover, nonchamber myocardium contains loosely arranged myofibrils and sarcoplasmic reticulum in contrast to the highly ordered contractile apparatus in chamber myocardium.

Summary of myocardial development

The process of making a functional myocardium is meticulous. It starts with the specification of the tissue lineage that will give rise to the contractile layer of the heart. What follows is a complicated progression of morphogenetic and differentiation events that will transform the bilateral set of precursor cells into a chambered, beating organ that propels oxygen- and nutrient-rich blood to circulate. Fundamental to this transformation are the differentiation of specialized regions of the heart tube to chamber myocardium and the maintenance of characteristics of the primitive tube in nonchamber myocardium. Despite the complexity of these events, there are two underlying themes. First, different events are orchestrated by the same signaling pathways that act differentially depending upon spatiotemporal control. Second, members of one signaling family can act in concert with or against other members to regulate the same result. In spite of advances in identifying these signaling pathways, elucidating how these pathways overlap and how they are integrated to result in the final output of a formed and functional heart remain a

challenge. This dissertation will provide insights to these questions in the context of heparan sulfate proteoglycans (HSPGs), biomolecules important for cell signaling and communication.

HSPGs

Developmental biologists first discovered the functional importance of HSPGs from genetic screens that isolated patterning defects in *Drosophila* and *C. elegans* (Herman and Horvitz, 1999; Bulik et al., 2000; Duncan et al., 2001; Filmus and Selleck, 2001). These studies corroborated what had already been gleaned of HSPG function from *in vitro* work. More significant is that they have emphasized the importance of HSPGs in core developmental processes including setting up morphogen gradients and growth factor signaling. This ability is a result of HSPG structure and its biosynthesis.

HSPGs are composed of cell surface or extracellular matrix (ECM) core proteins that have attachment sites for glycosaminoglycan (GAG) chains. The GAG chains in HSPGs are unbranched, charged polysaccharides composed of repeating disaccharide units of *N*-acetylglucosamine and glucuronic acid (Esko and Lindahl, 2001). These sugar chains are further modified through *N*-deacetylation/*N*-sulfation, epimerization, and O-sulfation. Not all sugar residues are modified, resulting in GAG chains with relatively small clusters of modified units interspersed with larger sections of unmodified units (Esko and Selleck, 2002). This results in an astounding level of structural heterogeneity, producing GAG chains with varying specificities for protein binding (Park et al., 2000). Most of the genes encoding the core proteins and the enzymes that synthesize and modify the GAG chains have been identified, and gene knockouts and knockdowns in various

animal models have elucidated their roles in development (Bulow and Hobert, 2006). In contrast how biosynthesis is controlled and regulated remains poorly understood.

Tissue-specific expression of the core proteins dictates spatiotemporal expression of GAG chains and the repertoire of modifying enzymes can also differ between cells (Park et al., 2000; Esko and Lindahl, 2001). This, in theory, could impact how a cell interacts with a ligand, a neighboring cell, or the ECM. The "glyco code" presented by these GAG chains is an essential level of regulation but is not well explored.

This dissertation will address the importance of 3-O-sulfation, one type of O-sulfation catalyzed by 3-O-sulfotransferases (3-OSTs), in zebrafish heart development. The biological function of this rare type of modification is poorly understood. Knockout of the 3-OST-1 gene in mouse resulted in intrauterine growth retardation and lethality in certain genetic backgrounds (Shworak et al., 2002; HajMohammadi et al., 2003). Because the existence of other 3-OST genes may have compensated for the loss of 3-OST-1, other phenotypes may have been masked. The role of 3-O-sulfation has also been studied in invertebrates where knockdown of 3-OST-B in Drosophila resulted in neurological phenotypes (Kamimura et al., 2004). Aside from these studies, no other *in vivo* function has been ascribed to 3-O-sulfation.

That 3-O-sulfation could modulate heart development is a tantalizing concept yet not too surprising. Given the functions that have been discovered for HSPGs in development, it is not far-fetched that this modification could add another level of regulation to the complex activities occurring during heart development. It could potentially provide insight as to how the different signaling pathways acting to form the heart are integrated to achieve that ultimate goal.

References

Abu-Issa R, Waldo K, Kirby ML (2004) Heart fields: one, two or more? Dev Biol 272:281-285.

Ai D, Fu X, Wang J, Lu MF, Chen L, Baldini A, Klein WH, Martin JF (2007) Canonical Wnt signaling functions in second heart field to promote right ventricular growth. Proc Natl Acad Sci U S A 104:9319-9324.

Arguello C, Alanis J, Valenzuela B (1988) The early development of the atrioventricular node and bundle of His in the embryonic chick heart. An electrophysiological and morphological study. Development 102:623-637.

Auman HJ, Coleman H, Riley HE, Olale F, Tsai HJ, Yelon D (2007) Functional modulation of cardiac form through regionally confined cell shape changes. PLoS Biol 5:e53.

Bakker ML, Boukens BJ, Mommersteeg MT, Brons JF, Wakker V, Moorman AF, Christoffels VM (2008) Transcription factor Tbx3 is required for the specification of the atrioventricular conduction system. Circ Res 102:1340-1349.

Berdougo E, Coleman H, Lee DH, Stainier DY, Yelon D (2003) Mutation of weak atrium/atrial myosin heavy chain disrupts atrial function and influences ventricular morphogenesis in zebrafish. Development 130:6121-6129.

Bers DM (2002) Cardiac excitation-contraction coupling. Nature 415:198-205.

Boateng SY, Goldspink PH (2008) Assembly and maintenance of the sarcomere night and day. Cardiovasc Res 77:667-675.

Brown DD, Martz SN, Binder O, Goetz SC, Price BM, Smith JC, Conlon FL (2005) Tbx5 and Tbx20 act synergistically to control vertebrate heart morphogenesis. Development 132:553-563.

Bruneau BG, Nemer G, Schmitt JP, Charron F, Robitaille L, Caron S, Conner DA, Gessler M, Nemer M, Seidman CE, Seidman JG (2001) A murine model of Holt-Oram syndrome defines roles of the T-box transcription factor Tbx5 in cardiogenesis and disease. Cell 106:709-721.

Buckingham M, Meilhac S, Zaffran S (2005) Building the mammalian heart from two sources of myocardial cells. Nat Rev Genet 6:826-835.

Bulik DA, Wei G, Toyoda H, Kinoshita-Toyoda A, Waldrip WR, Esko JD, Robbins PW, Selleck SB (2000) sqv-3, -7, and -8, a set of genes affecting morphogenesis in Caenorhabditis elegans, encode enzymes required for glycosaminoglycan biosynthesis. Proc Natl Acad Sci U S A 97:10838-10843.

Bulow HE, Hobert O (2006) The molecular diversity of glycosaminoglycans shapes animal development. Annu Rev Cell Dev Biol 22:375-407.

Cai CL, Liang X, Shi Y, Chu PH, Pfaff SL, Chen J, Evans S (2003) Isl1 identifies a cardiac progenitor population that proliferates prior to differentiation and contributes a majority of cells to the heart. Dev Cell 5:877-889.

Cai CL, Zhou W, Yang L, Bu L, Qyang Y, Zhang X, Li X, Rosenfeld MG, Chen J, Evans S (2005) T-box genes coordinate regional rates of proliferation and regional specification during cardiogenesis. Development 132:2475-2487.

Christoffels VM, Hoogaars WM, Tessari A, Clout DE, Moorman AF, Campione M (2004) T-box transcription factor Tbx2 represses differentiation and formation of the cardiac chambers. Dev Dyn 229:763-770.

Clark KA, McElhinny AS, Beckerle MC, Gregorio CC (2002) Striated muscle cytoarchitecture: an intricate web of form and function. Annu Rev Cell Dev Biol 18:637-706.

Cohen ED, Wang Z, Lepore JJ, Lu MM, Taketo MM, Epstein DJ, Morrisey EE (2007) Wnt/beta-catenin signaling promotes expansion of Isl-1-positive cardiac progenitor cells through regulation of FGF signaling. J Clin Invest 117:1794-1804.

Dabiri GA, Turnacioglu KK, Sanger JM, Sanger JW (1997) Myofibrillogenesis visualized in living embryonic cardiomyocytes. Proc Natl Acad Sci U S A 94:9493-9498.

de Pater E, Clijsters L, Marques SR, Lin YF, Garavito-Aguilar ZV, Yelon D, Bakkers J (2009) Distinct phases of cardiomyocyte differentiation regulate growth of the zebrafish heart. Development 136:1633-1641.

Dlugosz AA, Antin PB, Nachmias VT, Holtzer H (1984) The relationship between stress fiber-like structures and nascent myofibrils in cultured cardiac myocytes. J Cell Biol 99:2268-2278.

Du A, Sanger JM, Sanger JW (2008) Cardiac myofibrillogenesis inside intact embryonic hearts. Dev Biol 318:236-246.

Du A, Sanger JM, Linask KK, Sanger JW (2003) Myofibrillogenesis in the first cardiomyocytes formed from isolated quail precardiac mesoderm. Dev Biol 257:382-394.

Duncan G, McCormick C, Tufaro F (2001) The link between heparan sulfate and hereditary bone disease: finding a function for the EXT family of putative tumor suppressor proteins. J Clin Invest 108:511-516.

Ehler E, Fowler VM, Perriard JC (2004) Myofibrillogenesis in the developing chicken heart: role of actin isoforms and of the pointed end actin capping protein tropomodulin during thin filament assembly. Dev Dyn 229:745-755.

Ehler E, Rothen BM, Hammerle SP, Komiyama M, Perriard JC (1999) Myofibrillogenesis in the developing chicken heart: assembly of Z-disk, M-line and the thick filaments. J Cell Sci 112 (Pt 10):1529-1539.

Esko JD, Lindahl U (2001) Molecular diversity of heparan sulfate. J Clin Invest 108:169-173.

Esko JD, Selleck SB (2002) Order out of chaos: assembly of ligand binding sites in heparan sulfate. Annu Rev Biochem 71:435-471.

Evans SM, Yelon D, Conlon FL, Kirby ML (2010) Myocardial lineage development. Circ Res 107:1428-1444.

Filmus J, Selleck SB (2001) Glypicans: proteoglycans with a surprise. J Clin Invest 108:497-501.

Fromaget C, el Aoumari A, Gros D (1992) Distribution pattern of connexin 43, a gap junctional protein, during the differentiation of mouse heart myocytes. Differentiation 51:9-20.

Garry DJ, Olson EN (2006) A common progenitor at the heart of development. Cell 127:1101-1104.

Goddeeris MM, Rho S, Petiet A, Davenport CL, Johnson GA, Meyers EN, Klingensmith J (2008) Intracardiac septation requires hedgehog-dependent cellular contributions from outside the heart. Development 135:1887-1895.

Gordon AM, Regnier M, Homsher E (2001) Skeletal and cardiac muscle contractile activation: tropomyosin "rocks and rolls". News Physiol Sci 16:49-55.

Gourdie RG, Green CR, Severs NJ, Thompson RP (1992) Immunolabelling patterns of gap junction connexins in the developing and mature rat heart. Anat Embryol (Berl) 185:363-378.

Gros D, Jarry-Guichard T, Ten Velde I, de Maziere A, van Kempen MJ, Davoust J, Briand JP, Moorman AF, Jongsma HJ (1994) Restricted distribution of connexin40, a gap junctional protein, in mammalian heart. Circ Res 74:839-851.

Habets PE, Moorman AF, Clout DE, van Roon MA, Lingbeek M, van Lohuizen M, Campione M, Christoffels VM (2002) Cooperative action of Tbx2 and Nkx2.5 inhibits ANF expression in the atrioventricular canal: implications for cardiac chamber formation. Genes Dev 16:1234-1246.

HajMohammadi S, Enjyoji K, Princivalle M, Christi P, Lech M, Beeler D, Rayburn H, Schwartz JJ, Barzegar S, de Agostini AI, Post MJ, Rosenberg RD, Shworak NW (2003) Normal levels of anticoagulant heparan sulfate are not essential for normal hemostasis. J Clin Invest 111:989-999.

Herman T, Horvitz HR (1999) Three proteins involved in Caenorhabditis elegans vulval invagination are similar to components of a glycosylation pathway. Proc Natl Acad Sci U S A 96:974-979.

Holtzer H, Hijikata T, Lin ZX, Zhang ZQ, Holtzer S, Protasi F, Franzini-Armstrong C, Sweeney HL (1997) Independent assembly of 1.6 microns long bipolar MHC filaments and I-Z-I bodies. Cell Struct Funct 22:83-93.

Hoogaars WM, Barnett P, Moorman AF, Christoffels VM (2007) T-box factors determine cardiac design. Cell Mol Life Sci 64:646-660.

Huang C, Sheikh F, Hollander M, Cai C, Becker D, Chu PH, Evans S, Chen J (2003) Embryonic atrial function is essential for mouse embryogenesis, cardiac morphogenesis and angiogenesis. Development 130:6111-6119.

Huang W, Zhang R, Xu X (2009) Myofibrillogenesis in the developing zebrafish heart: A functional study of tnnt2. Dev Biol 331:237-249.

Jiao K, Kulessa H, Tompkins K, Zhou Y, Batts L, Baldwin HS, Hogan BL (2003) An essential role of Bmp4 in the atrioventricular septation of the mouse heart. Genes Dev 17:2362-2367.

Kamimura K, Rhodes JM, Ueda R, McNeely M, Shukla D, Kimata K, Spear PG, Shworak NW, Nakato H (2004) Regulation of Notch signaling by Drosophila heparan sulfate 3-O sulfotransferase. J Cell Biol 166:1069-1079.

Kelly RG, Brown NA, Buckingham ME (2001) The arterial pole of the mouse heart forms from Fgf10-expressing cells in pharyngeal mesoderm. Dev Cell 1:435-440.

Kwon C, Arnold J, Hsiao EC, Taketo MM, Conklin BR, Srivastava D (2007) Canonical Wnt signaling is a positive regulator of mammalian cardiac progenitors. Proc Natl Acad Sci U S A 104:10894-10899.

Laugwitz KL, Moretti A, Lam J, Gruber P, Chen Y, Woodard S, Lin LZ, Cai CL, Lu MM, Reth M, Platoshyn O, Yuan JX, Evans S, Chien KR (2005) Postnatal isl1+ cardioblasts enter fully differentiated cardiomyocyte lineages. Nature 433:647-653.

Liao J, Aggarwal VS, Nowotschin S, Bondarev A, Lipner S, Morrow BE (2008) Identification of downstream genetic pathways of Tbx1 in the second heart field. Dev Biol 316:524-537.

Ma L, Lu MF, Schwartz RJ, Martin JF (2005) Bmp2 is essential for cardiac cushion epithelial-mesenchymal transition and myocardial patterning. Development 132:5601-5611.

Mandel EM, Kaltenbrun E, Callis TE, Zeng XX, Marques SR, Yelon D, Wang DZ, Conlon FL (2010) The BMP pathway acts to directly regulate Tbx20 in the developing heart. Development 137:1919-1929.

Marques SR, Yelon D (2009) Differential requirement for BMP signaling in atrial and ventricular lineages establishes cardiac chamber proportionality. Dev Biol 328:472-482.

Marques SR, Lee Y, Poss KD, Yelon D (2008) Reiterative roles for FGF signaling in the establishment of size and proportion of the zebrafish heart. Dev Biol 321:397-406.

Mesbah K, Harrelson Z, Theveniau-Ruissy M, Papaioannou VE, Kelly RG (2008) Tbx3 is required for outflow tract development. Circ Res 103:743-750.

Ojima K, Lin ZX, Zhang ZQ, Hijikata T, Holtzer S, Labeit S, Sweeney HL, Holtzer H (1999) Initiation and maturation of I-Z-I bodies in the growth tips of transfected myotubes. J Cell Sci 112 (Pt 22):4101-4112.

Parameswaran M, Tam PP (1995) Regionalisation of cell fate and morphogenetic movement of the mesoderm during mouse gastrulation. Dev Genet 17:16-28.

Park C, Lavine K, Mishina Y, Deng CX, Ornitz DM, Choi K (2006) Bone morphogenetic protein receptor 1A signaling is dispensable for hematopoietic development but essential for vessel and atrioventricular endocardial cushion formation. Development 133:3473-3484.

Park PW, Reizes O, Bernfield M (2000) Cell surface heparan sulfate proteoglycans: selective regulators of ligand-receptor encounters. J Biol Chem 275:29923-29926.

Phillips HM, Murdoch JN, Chaudhry B, Copp AJ, Henderson DJ (2005) Vangl2 acts via RhoA signaling to regulate polarized cell movements during development of the proximal outflow tract. Circ Res 96:292-299.

Qyang Y, Martin-Puig S, Chiravuri M, Chen S, Xu H, Bu L, Jiang X, Lin L, Granger A, Moretti A, Caron L, Wu X, Clarke J, Taketo MM, Laugwitz KL, Moon RT, Gruber P, Evans SM, Ding S, Chien KR (2007) The renewal and differentiation of Isl1+ cardiovascular progenitors are controlled by a Wnt/beta-catenin pathway. Cell Stem Cell 1:165-179.

Raffin M, Leong LM, Rones MS, Sparrow D, Mohun T, Mercola M (2000) Subdivision of the cardiac Nkx2.5 expression domain into myogenic and nonmyogenic compartments. Dev Biol 218:326-340.

Reifers F, Walsh EC, Leger S, Stainier DY, Brand M (2000) Induction and differentiation of the zebrafish heart requires fibroblast growth factor 8 (fgf8/acerebellar). Development 127:225-235.

Reiter JF, Verkade H, Stainier DY (2001) Bmp2b and Oep promote early myocardial differentiation through their regulation of gata5. Dev Biol 234:330-338.

Rhee D, Sanger JM, Sanger JW (1994) The premyofibril: evidence for its role in myofibrillogenesis. Cell Motil Cytoskeleton 28:1-24.

Rottbauer W, Baker K, Wo ZG, Mohideen MA, Cantiello HF, Fishman MC (2001) Growth and function of the embryonic heart depend upon the cardiac-specific L-type calcium channel alpha1 subunit. Dev Cell 1:265-275.

Rottbauer W, Wessels G, Dahme T, Just S, Trano N, Hassel D, Burns CG, Katus HA, Fishman MC (2006) Cardiac myosin light chain-2: a novel essential component of thick-myofilament assembly and contractility of the heart. Circ Res 99:323-331.

Rutenberg JB, Fischer A, Jia H, Gessler M, Zhong TP, Mercola M (2006) Developmental patterning of the cardiac atrioventricular canal by Notch and Hairy-related transcription factors. Development 133:4381-4390.

Sanger JW, Kang S, Siebrands CC, Freeman N, Du A, Wang J, Stout AL, Sanger JM (2005) How to build a myofibril. J Muscle Res Cell Motil 26:343-354.

Schoenebeck JJ, Keegan BR, Yelon D (2007) Vessel and blood specification override cardiac potential in anterior mesoderm. Dev Cell 13:254-267.

Schultheiss T, Lin ZX, Lu MH, Murray J, Fischman DA, Weber K, Masaki T, Imamura M, Holtzer H (1990) Differential distribution of subsets of myofibrillar proteins in cardiac nonstriated and striated myofibrils. J Cell Biol 110:1159-1172.

Sehnert AJ, Huq A, Weinstein BM, Walker C, Fishman M, Stainier DY (2002) Cardiac troponin T is essential in sarcomere assembly and cardiac contractility. Nat Genet 31:106-110.

Shi Y, Katsev S, Cai C, Evans S (2000) BMP signaling is required for heart formation in vertebrates. Dev Biol 224:226-237.

Shworak NW, HajMohammadi S, de Agostini AI, Rosenberg RD (2002) Mice deficient in heparan sulfate 3-O-sulfotransferase-1: normal hemostasis with unexpected perinatal phenotypes. Glycoconj J 19:355-361.

Singh MK, Christoffels VM, Dias JM, Trowe MO, Petry M, Schuster-Gossler K, Burger A, Ericson J, Kispert A (2005) Tbx20 is essential for cardiac chamber differentiation and repression of Tbx2. Development 132:2697-2707.

Solaro RJ, Rarick HM (1998) Troponin and tropomyosin: proteins that switch on and tune in the activity of cardiac myofilaments. Circ Res 83:471-480.

Srivastava D (2006) Making or breaking the heart: from lineage determination to morphogenesis. Cell 126:1037-1048.

Stainier DY, Fishman MC (1994) The zebrafish as a model system to study cardiovascular development. Trends Cardiovasc Med 4:207-212.

Stalsberg H, DeHaan RL (1969) The precardiac areas and formation of the tubular heart in the chick embryo. Dev Biol 19:128-159.

Stennard FA, Costa MW, Lai D, Biben C, Furtado MB, Solloway MJ, McCulley DJ, Leimena C, Preis JI, Dunwoodie SL, Elliott DE, Prall OW, Black BL, Fatkin D, Harvey RP (2005) Murine T-box transcription factor Tbx20 acts as a repressor during heart development, and is essential for adult heart integrity, function and adaptation. Development 132:2451-2462.

Stern MD (1992) Theory of excitation-contraction coupling in cardiac muscle. Biophys J 63:497-517.

Thomas NA, Koudijs M, van Eeden FJ, Joyner AL, Yelon D (2008) Hedgehog signaling plays a cell-autonomous role in maximizing cardiac developmental potential. Development 135:3789-3799.

Tobacman LS (1996) Thin filament-mediated regulation of cardiac contraction. Annu Rev Physiol 58:447-481.

van Kempen MJ, Fromaget C, Gros D, Moorman AF, Lamers WH (1991) Spatial distribution of connexin43, the major cardiac gap junction protein, in the developing and adult rat heart. Circ Res 68:1638-1651.

Vibert P, Craig R, Lehman W (1997) Steric-model for activation of muscle thin filaments. J Mol Biol 266:8-14.

Walters MJ, Wayman GA, Christian JL (2001) Bone morphogenetic protein function is required for terminal differentiation of the heart but not for early expression of cardiac marker genes. Mech Dev 100:263-273.

Wiese C, Grieskamp T, Airik R, Mommersteeg MT, Gardiwal A, de Gier-de Vries C, Schuster-Gossler K, Moorman AF, Kispert A, Christoffels VM (2009) Formation of the sinus node head and differentiation of sinus node myocardium are independently regulated by Tbx18 and Tbx3. Circ Res 104:388-397.

Xu X, Meiler SE, Zhong TP, Mohideen M, Crossley DA, Burggren WW, Fishman MC (2002) Cardiomyopathy in zebrafish due to mutation in an alternatively spliced exon of titin. Nat Genet 30:205-209.

Yang L, Cai CL, Lin L, Qyang Y, Chung C, Monteiro RM, Mummery CL, Fishman GI, Cogen A, Evans S (2006) Isl1Cre reveals a common Bmp pathway in heart and limb development. Development 133:1575-1585.

Yelon D, Horne SA, Stainier DY (1999) Restricted expression of cardiac myosin genes reveals regulated aspects of heart tube assembly in zebrafish. Dev Biol 214:23-37.

Zhao L, Zhao X, Tian T, Lu Q, Skrbo-Larssen N, Wu D, Kuang Z, Zheng X, Han Y, Yang S, Zhang C, Meng A (2008) Heart-specific isoform of tropomyosin4 is essential for heartbeat in zebrafish embryos. Cardiovasc Res 80:200-208.

Zhou W, Lin L, Majumdar A, Li X, Zhang X, Liu W, Etheridge L, Shi Y, Martin J, Van de Ven W, Kaartinen V, Wynshaw-Boris A, McMahon AP, Rosenfeld MG, Evans SM (2007) Modulation of morphogenesis by noncanonical Wnt signaling requires ATF/CREB family-mediated transcriptional activation of TGFbeta2. Nat Genet 39:1225-1234.

CHAPTER 2

3-OST-7 REGULATES MYOFIBRILLOGENESIS TO CONTROL HEART CONTRACTION IN ZEBRAFISH

Abstract

3-O-sulfation is a rare and specific modification of glycosaminoglycan chains on heparan sulfate proteoglycans catalyzed by a family of 3-O-sulfotransferases (3-OSTs). Despite gene expression studies suggesting distinct roles for different members of the 3-OST family in embryonic development, we have limited understanding of *in vivo* functions of this type of modification. In this study we demonstrate that 3-OST-7 regulates cardiac development in zebrafish. Morpholino knockdown of 3-OST-7 resulted in ventricular noncontraction, and was rescued by ubiquitous overexpression of 3-OST-7 in transgenic zebrafish. Cardiac precursor cells were specified correctly, and atrial and ventricular cardiomyocytes had normal action potentials and calcium transients, indicating the noncontractile ventricle undergoes normal excitation cycling. In contrast, 3-OST-7 morphants had aberrant sarcomere assembly, thus uncoupling contraction from excitation. Moreover, transcription of a sarcomeric gene, *tropomyosin4* (*tpm4*), was donwregulated in 3-OST-7 morphants. Strikingly, overexpression of *tpm4* was capable of rescuing ventricular noncontraction in 3-OST-7 morphants, indicating 3-OST-7 is required for transcription of *tpm4*, which then ensures functional levels of Tpm4 and other proteins in the sarcomere. Together these results revealed 3-OST-7 as the first

member of a novel pathway in cardiac development that regulates transcription of *tpm4*, and coordinates sarcomere assembly and ventricle function.

Introduction

Vertebrate heart development is a complex process. It begins with events that specify the endocardial and myocardial lineages, which are then organized in a specific design to render it functional (Stainier, 2001; Glickman and Yelon, 2002). After gastrulation, myocardial precursors are situated in bilateral positions in the anterior lateral plate mesoderm (LPM). Through expression of genes encoding sarcomere proteins, such as cardiac myosin light chain 2 (cmlc2), these precursor cells initiate differentiation (Yelon et al., 1999). While differentiation and morphogenetic events transform the bilateral set of precursors into the heart tube, the primitive heart also begins to function. A molecular framework has emerged that elucidates the commitment of exclusive lineages to discrete regions of the heart, and the underlying cellular decisions that direct the three-dimensional events of cardiac formation (Evans et al., 2010; Noseda et al., 2011). Despite these advances in our understanding of heart development, critical questions remain in the field and unknown players remain to be discovered. In this study, we focus on the role of heparan sulfate proteoglycans (HSPGs) in heart development.

HSPGs are cell surface and extracellular matrix molecules composed of a core protein to which glycosaminoglycan (GAG) chains are covalently linked. Their location and the ability of HSPGs to interact with signaling ligands and receptors and extracellular matrix (ECM) components place them at a unique advantage to modulate complex biological processes such as morphogenesis, tissue repair and host defense (Park et al., 2000; Hacker et al., 2005; Lamanna et al., 2007).

The specificity of interactions of an HSPG and its environment is due, in part, to the GAG chains (Lin, 2004; Bulow and Hobert, 2006; Lamanna et al., 2007). The GAG chains in HSPGs are unbranched, charged polysaccharides composed of repeating disaccharide units of *N*-acetylglucosamine and glucuronic acid. These chains are subjected to several kinds of modifications: *N*-deacetylation/*N*-sulfation, epimerization, and O-sulfation. Not all sugar residues are modified, resulting in GAG chains with relatively small clusters of modified units interspersed between large sections of unmodified units (Esko and Selleck, 2002). This gives rise to an astounding level of structural heterogeneity, producing GAG chains with varying specificities for protein binding (Park et al., 2000). The repertoire of modifying enzymes differs between cells (Park et al., 2000), which in theory could impact how a cell interacts with a ligand, a neighboring cell, or the ECM. Previous gene knockdown and knockout studies have already documented the roles of these modifying enzymes (Bulow and Hobert, 2006), but none has been implicated in heart development.

In this study, we focus on a rare and specific kind of O-sulfation, 3-O-sulfation, performed by a family of enzymes, the 3-O-sulfotransferases (3-OSTs). 3-OSTs catalyze transfer of a sulfate group to the hydroxyl of the third carbon of *N*-sulfated glucosamine residues (Esko and Selleck, 2002). Previous work in our lab has identified and cloned the 3-OST family in zebrafish (Cadwallader and Yost, 2006b). Gene expression analysis reveals dynamic spatial and temporal expression patterns for the eight 3-OST family members suggesting distinct roles in the developing embryo.

Here we show that morpholino knockdown of one of eight 3-OSTs in zebrafish, 3-OST-7, gives a specific cardiac phenotype at 48 hours postfertilization (hpf). 3-OST-7

is expressed ubiquitously early in development (Cadwallader and Yost, 2006b), but morpholino knockdown results in a noncontracting ventricle. Examining this 3-OST-7 knockdown model demonstrates myofibrillogenesis is dependent on 3-OST-7 and that ventricular noncontraction occurs because of uncoupling of contraction from excitation due to aberrant sarcomeres. Results show that the noncontractile ventricle in 3-OST-7 morphant zebrafish can be rescued by overexpression of a sarcomeric protein, tropomyosin4 (Tpm4). This indicates that 3-OST-7 is required for myofibrillogenesis, providing a novel mechanism for the regulation of cardiac cell physiology.

Results

Cardiac ventricle contraction requires 3-OST-7

To begin elucidating the role of 3-OST-7 in development, we injected two different antisense morpholinos (MO) to block protein expression. Zebrafish embryos injected with either a translation-blocking (MO1) or a splice-blocking (MO2) MO had no perceived gross morphological difference from control embryos until 48 hpf, at which stage pericardial edema and blood pooling became obvious in 3-OST-7 morphants (Figure 2.1A and 2.1B). These classic indications of a cardiovascular defect prompted a closer inspection of the heart. Visualizing the heart using transgenic *Tg(cmlc2:gfp)* zebrafish (Huang et al., 2003) revealed that 3-OST-7 morphants have a hypoplastic cardiac ventricle that does not contract properly (Figure 2.1F and 2.1G, and Supplemental Movie 2.2), resulting in poor blood circulation (Figure 2.1H, Supplemental Movie 2.4). In contrast, a control embryo, had a clearly contractile ventricle, which undergoes sequential diastole (Figure 2.1C) and systole (Figure 2.1D). The atrium of 3-OST-7

morphants, on the other hand, was contracting and looked similar to control (Figure 2.1C, 2.1D, 2.1F, and 2.1G).

To test whether the noncontracting ventricle phenotype in 3-OST-7 morphants was specifically due to MO knockdown of 3-OST-7, we attempted to rescue the phenotype by injection of 3-OST-7 mRNA that does not bind MO. This approach was not successful in rescuing the phenotype (data not shown), perhaps due to issues of mRNA or protein stability, prompting us to create stable transgenic zebrafish lines expressing 3-OST-7 ubiquitously or in a heart-specific manner. Utilizing the Tol2kit cloning system (Kwan et al., 2007), we made transgenic zebrafish overexpressing 3-OST-7 under the control of the β-actin promoter for ubiquitous expression (*Tg(β-actin:3-OST-7)*) or the cmlc2 promoter for heart-specific expression (*Tg(cmlc2:3-OST-7)*). The MO binding sequence is not present in either construct so that MO would not inhibit transgenic expression of 3-OST-7. Both transgenes had a 3' IRES-EGFP-polyA tag downstream of 3-OST-7 coding region, enabling identification of zebrafish overexpressing 3-OST-7 by co-expression of GFP. We observed significant rescue of the noncontractile ventricle in transgenic *Tg(β-actin:3-OST-7-IRES-EGFP)* embryo (Figure 2.1I), but not in *Tg(cmlc2:3-OST-7-IRES-EGFP)* (Figure 2.1J). Rescue of the noncontracting ventricle phenotype by ubiquitous overexpression of 3-OST-7 in *Tg(β-actin:3-OST-7-IRES-EGFP)* embryo demonstrates the noncontracting ventricle phenotype is specific to knockdown of 3-OST-7. Moreover, rescue in *Tg(β-actin:3-OST-7-IRES-EGFP)* embryo and not in *Tg(cmlc2:3-OST-7-EGFP)* embryo suggests either a spatial or a temporal requirement for 3-OST-7 beyond the expression driven by the *cmlc2* promoter.

Figure 2.1. 3-OST-7 is required for ventricular contraction in the zebrafish heart. Lateral views of control (uninjected, wild-type) (A) and 3-OST-7 morphant (B) embryos at 48 hpf showing edema (red arrowhead) and blood pooling (black arrowhead) with knockdown of 3-OST-7. Lateral views of hearts in control (C and D) and 3-OST-7 morphants (injected with 3-OST-7 MO2) (F and G) *Tg(cmlc2:gfp)* embryos at periods of ventricular diastole (C and F) and systole (D and G). Dorsal aorta in control (E) and 3-OST-7 morphant (H) embryos show blood cells (red boxes) were not circulating normally in morphants. (I) Injection of 3-OST-7 MO2 in *Tg(β-actin:3-OST-7-IRES-EGFP)* embryos rescued the noncontractile ventricle phenotype ($P<0.039$). (J) Injection of same 3-OST-7 MO did not rescue the phenotype in *Tg(cmlc2:3-OST-7-IRES-EGFP)* *(*$P<0.601$). Graphs depict the percentage of embryos with phenotype in 3-OST-7-overexpressing (GFP+, green bar) or non-3-OST-7-overexpressing (GFP-, white) embryos from individual crosses between one of three transgenic founders and wild-type AB zebrafish (TF x AB). At, atrium; V, ventricle.

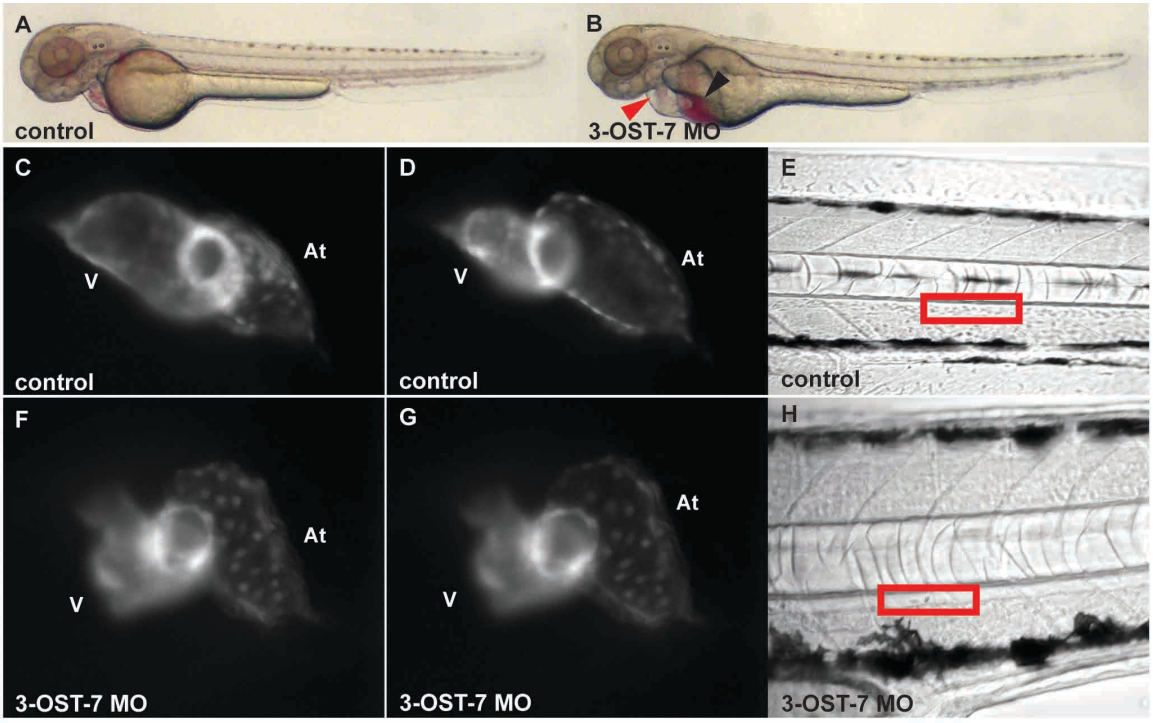
A
control
B
3-OST-7 MO
C
At
V
control
D
At
V
control
E
control
F
At
V
3-OST-7 MO
G
At
V
3-OST-7 MO
H
3-OST-7 MO
I
Tg(β-actin:3-OST-7-IRES-EGFP)
Percentage of Embryos with Noncontracting Ventricle
GFP-
GFP+
100
80
60
40
20
TF1 x AB
TF2 x AB
TF3 x AB
n = 60 20 45 13 61 12
J
Tg(cmlc2:3-OST-7-IRES-EGFP)
Percentage of Embryos with Noncontracting Ventricle
GFP-
GFP+
100
80
60
40
20
TF4 x AB
TF5 x AB
TF6 x AB
n = 39 30 16 15 16 18

Heart field is specified correctly in 3-OST-7 morphants

A fully formed and functional heart is generated by the precise coordination of patterning events and cell movements. This complex process begins with the specification of cardiac cell precursors of myocardial and endocardial lineages, overall termed the heart field (Stainier, 2001; Glickman and Yelon, 2002). To determine whether the noncontracting ventricle in 3-OST-7 morphants is a result of aberrant heart field specification, we used several techniques to visualize the heart field to assess whether it is correctly specified in 3-OST-7 morphants. First we performed in situ hybridizations using markers for the cardiac precursor cells and the anterior LPM, tissue from which these cells arise. Combinatorial expression of the transcription factors *hand2* and *nkx2.5* serves as a marker for cardiac precursor cells (Schoenebeck et al., 2007). Expression of the LPM marker, *hand2*, in 3-OST-7 morphants was comparable to uninjected zebrafish (Figure 2.2A and 2.2B) and indicated that the anterior LPM was unaltered in 3-OST-7 morphants. Similarly *nkx2.5* was unaltered in 3-OST-7 morphants (Figure 2.2C and 2.2D). Furthermore a marker for myocardial precursors, *cmlc2*, was also expressed normally in 3-OST-7 morphants (Figure 2.2E and 2.2F). Next we used transgenic *Tg(fli1:EGFP)* embryos (Lawson and Weinstein, 2002) to examine the endocardial precursor cells and found that these cells were patterned similarly in control embryos and 3-OST-7 morphants (Figure 2.2G and 2.2H). In situ hybridizations for *amhc* (Figure 2.2I and 2.2J) and *vmhc* (Figure 2.2K and 2.2L), markers for myocardial precursors of the atrial and ventricular lineages, respectively, also indicated atrial and ventricular precursors were intact in 3-OST-7 morphants. Together these results

Figure 2.2. Heart field specification proceeds normally in 3-OST-7 morphants. Dorsal views (anterior on top) of control (uninjected, wild-type) (A, C, E and K), control MO (injected with control 3-OST-3Z MO) (G and I) and 3-OST-7 morphant (B, D, F, H, J and L) embryos; n=35 for each group. *In situ* hybridizations for: lateral plate mesoderm marker *hand2* (A and B, 17 hpf) and cardiac precursor cell marker *nkx2.5* (C and D, 17 hpf), myocardial precursor cell marker *cmlc2* (E and F, 17 hpf), atrial precursor cell marker *amhc* (I and J, 20 hpf), and ventricular precursor cell marker *vmhc* (K and L, 18 hpf) showing comparable levels and patterns of expression in control and 3-OST-7 morphant embryos. Imaging of *fli1* expression in *Tg(fli1:EGFP)* zebrafish at 18 hpf revealed endocardial lineage in intact in 3-OST-7 morphant embryos (G and H).

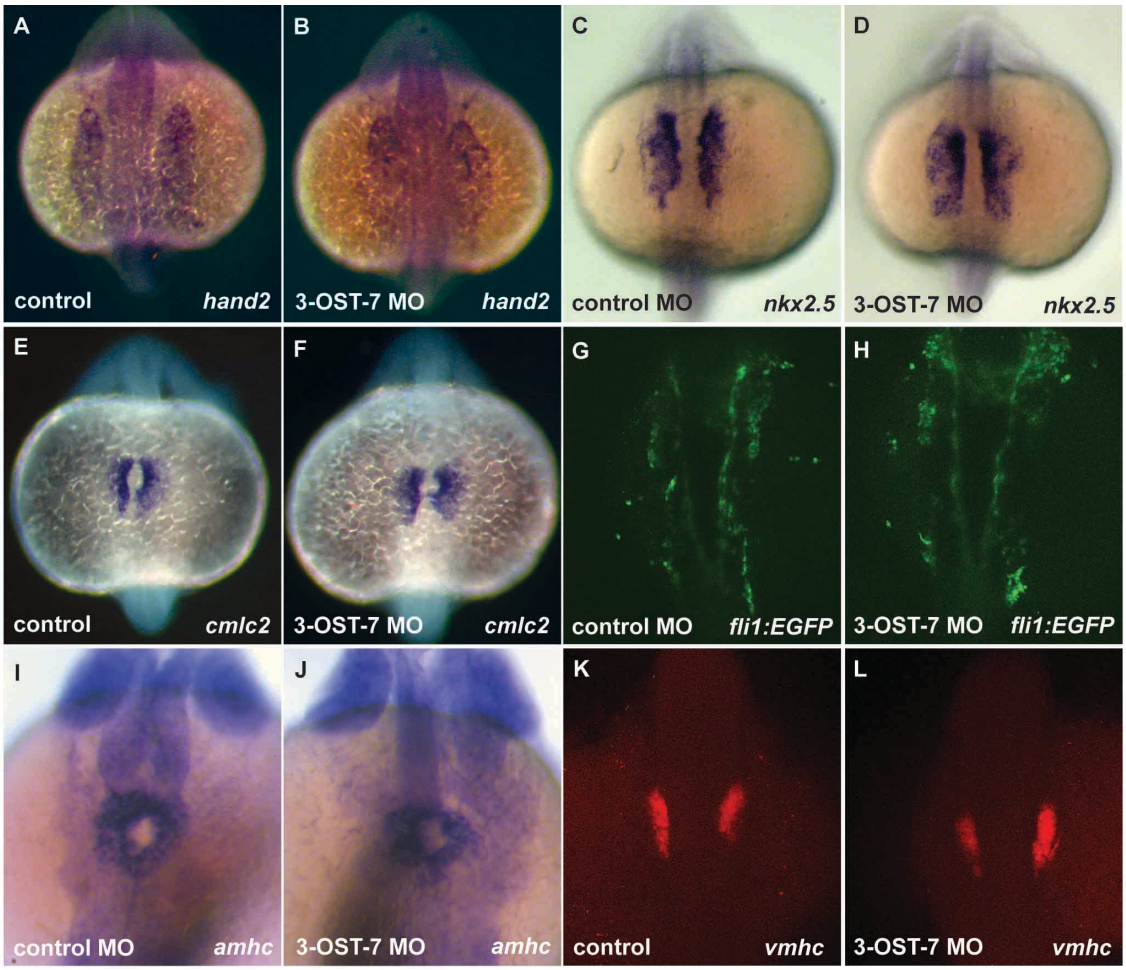
A
control
hand2
B
3-OST-7 MO
hand2
C
control MO
nkx2.5
D
3-OST-7 MO
nkx2.5
E
control
cmlc2
F
3-OST-7 MO
cmlc2
G
control MO
fli1:EGFP
H
3-OST-7 MO
fli1:EGFP
I
control MO
amhc
J
3-OST-7 MO
amhc
K
control
vmhc
L
3-OST-7 MO
vmhc

demonstrate heart field specification proceeds normally in 3-OST-7 morphants and is not likely the cause for the noncontracting ventricle.

Noncontracting ventricle in 3-OST-7 morphants generates action potentials

A fully functional heart characteristically undergoes excitation-contraction coupling process, a physiological process whereby an electrical stimulus (action potential) is converted to a mechanical response (contraction) (Stern, 1992). To determine whether the noncontracting ventricle in 3-OST-7 morphants results from uncoupling of contraction from excitation, we assessed whether the morphant ventricle could generate action potentials and calcium transients. To record action potentials, we performed patch clamp analysis on either the atrium or ventricle of hearts that were explanted from zebrafish embryos at 48 hpf (Figure 2.3A and 2.3B). As expected, atria of 3-OST-7 morphants were able to generate action potentials comparable to atria of control embryos (Figure 2.3C and 2.3D). Surprisingly, however, action potentials were also recorded for the noncontracting ventricles of 3-OST-7 morphants and these action potentials were similar to those recorded for ventricles of control embryos (Figure 2.3E and 2.3F). Moreover, analysis of action potential parameters revealed that there were no statistically significant differences between control embryos and 3-OST-7 morphants (data not shown). This demonstrates the ability of 3-OST-7 morphant ventricles to be electrically stimulated to generate action potentials. Specifically this indicates ion channels responsible for generating and propagating these action potentials were intact in 3-OST-7 morphants.

Figure 2.3. Noncontracting ventricle in 3-OST-7 morphants generates normal action potentials. (A) Zebrafish embryos were injected with 5.4 ng of 3-OST-7 MO1 at one-cell stage and allowed to develop until 48 hpf. The heart was then dissected out of the embryo and placed in a recording chamber perfused with solution containing 140 mM NaCl, 4 mM KCl, 1.8 mM $CaCl_2$, 1 mM $MgCl_2$, 10 mM glucose, and 10 mM Hepes (pH 7.4). (B) A suction pipette was used to patch clamp the heart at the atrial or ventricular region. Action potentials were recorded from atria (C and D) and ventricles (E and F) of control (uninjected, WT) (C and E) and 3-OST-7 morphant (D and F) embryos. The action potentials were comparable between control and 3-OST-7 morphant embryos. b.a., bulbus arteriosus.

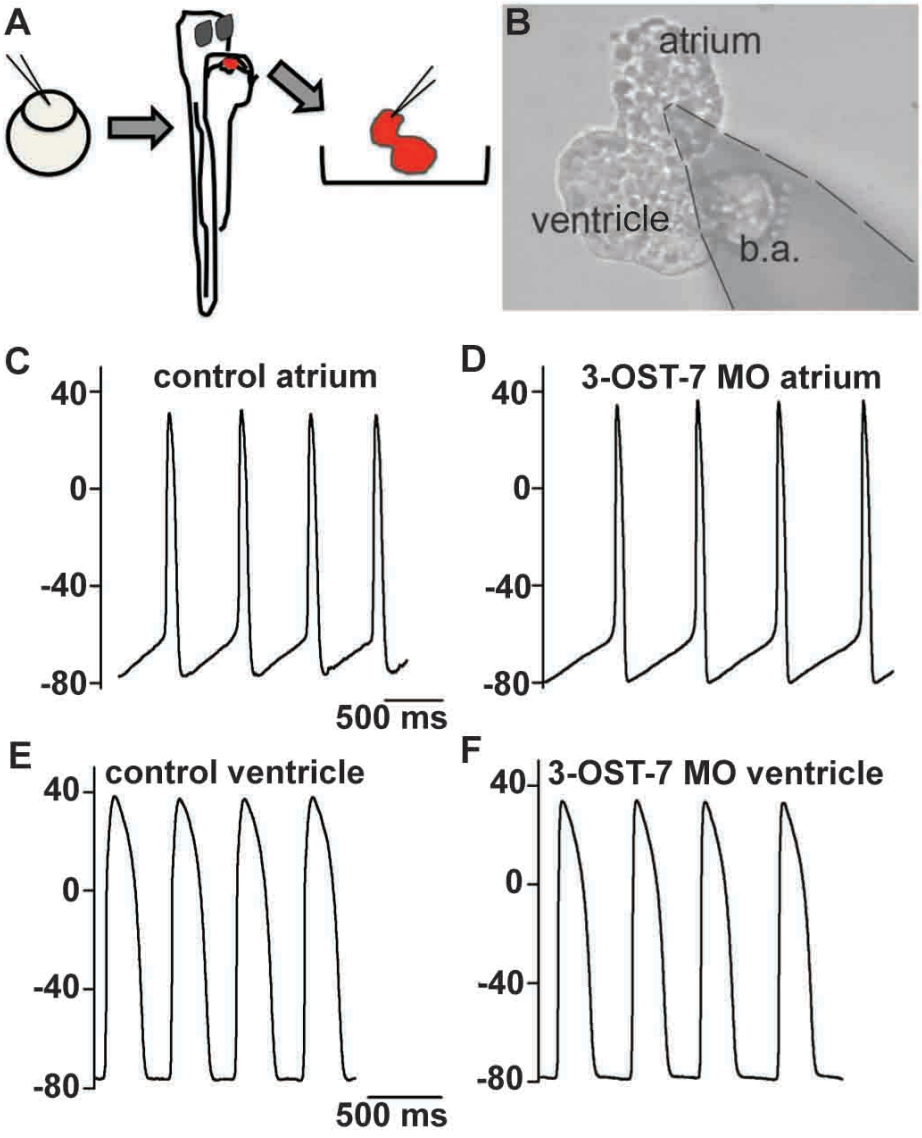
A
B
atrium
ventricle
b.a.
C
control atrium
40
0
-40
-80
500 ms
D
3-OST-7 MO atrium
40
0
-40
-80
E
control ventricle
40
0
-40
-80
500 ms
F
3-OST-7 MO ventricle
40
0
-40
-80

Noncontracting ventricle in 3-OST-7 morphants generates calcium transients

Once a myocardial cell has been stimulated by action potentials, this electrical signal is transduced intracellularly by the release of calcium ions from the sarcoplasmic reticulum (Bers, 2002). To assess whether this release occurs in 3-OST-7 morphant ventricles, we used two different techniques to image the calcium waves that occur during this process. In the first technique, we explanted hearts of zebrafish embryos and bathed them in the calcium indicator Fluo-4. These were then imaged by confocal microscopy and cardiac regions were selected to record the calcium transients and measure amplitude and time of decay. Comparable calcium waves were detected in hearts of both control embryos and 3-OST-7 morphants (Supplemental Movies 2.5 and 2.6). The 3-OST-7 morphant ventricles generated calcium transients similar to those generated by ventricles from control embryos (Figure 2.4C and 2.4D). There were no significant differences in the calcium transient amplitude and calcium transient decay between ventricles of 3-OST-7 morphant embryos and ventricles of control embryos (Figure 2.4E and 2.4F).

In the second technique, 3-OST-7 MO or control MO was injected into transgenic *Tg(cmlc2:gCaMP)*^{s878} embryos (Chi et al., 2008) that allowed for live calcium imaging in intact zebrafish. Similar to the other technique, calcium waves were detected in 3-OST-7 morphant hearts (Supplemental Movies 2.7 and 2.8) and comparable optical maps were generated for both control embryos and 3-OST-7 morphants (Figure 2.4G and 2.4H). There were no observed differences in conduction velocity.

Figure 2.4. Noncontracting ventricle in 3-OST-7 morphants generates calcium transients. Zebrafish was injected with 3-OST-7 MO1 or control 3-OST-5 MO at one-cell stage and allowed to develop until 48 hpf. The heart was then dissected out of the embryo, incubated in Fluo-4, and imaged using a confocal microscope. Regions were selected from atrium and ventricle to record the calcium transients (A-D) and measure the Ca^{2+} transient amplitude (E) and Ca^{2+} transient decay (F). No significant difference was detected between control and 3-OST-7 morphant embryos ($P<0.30$ for atrial transient amplitude; $P<0.16$ for ventricular transient amplitude; $P<0.37$ for atrial transient decay; and $P<0.51$ for ventricular transient decay). Using a different technique to image the calcium transients, 3-OST-7 MO1 or control 3-OST-3Z MO was injected into *Tg(cmlc2:gCaMP)*^{s878} embryos at one-cell stage and allowed to develop until 48 hpf. Optical maps of calcium activation for a single cycle, represented by isochronal lines every 20 ms, show calcium activation and conduction velocity proceed normally in 3-OST-7 morphants (H) compared to control MO injected embryos (G). Conduction proceeds from the atrium through the atrioventricular (AV) canal to the ventricle and numbers indicate the temporal sequence of calcium activation. Color bar chart fluorescence intensity changes on a scale of 0 to 100.

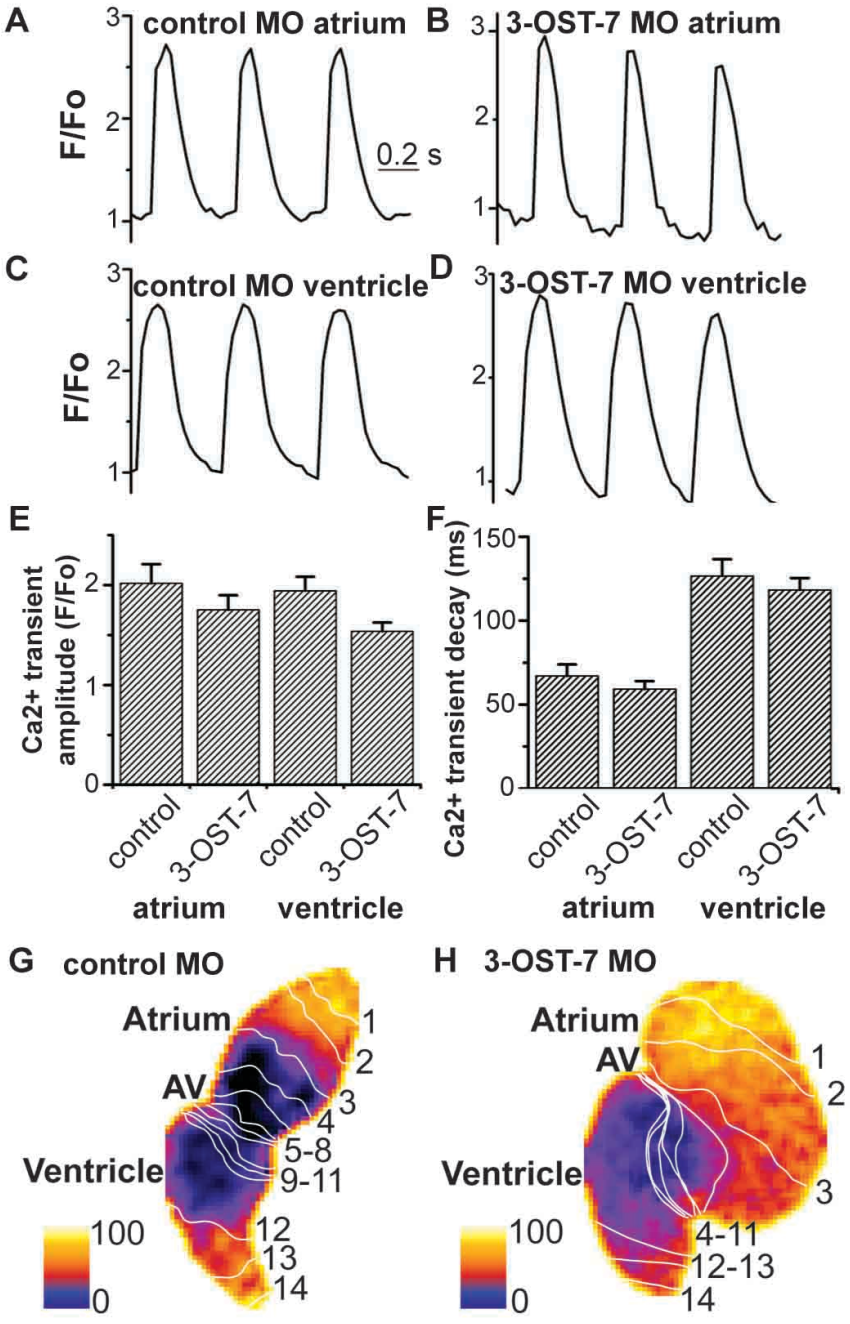
A
control MO atrium
F/Fo
0.2 s
B
3-OST-7 MO atrium
C
control MO ventricle
D
3-OST-7 MO ventricle
E
Ca2+ transient amplitude (F/Fo)
control
3-OST-7
control
3-OST-7
atrium
ventricle
F
Ca2+ transient decay (ms)
control
3-OST-7
control
3-OST-7
atrium
ventricle
G
control MO
Atrium
AV
Ventricle
1
2
3
4
5-8
9-11
12
13
14
100
0
H
3-OST-7 MO
Atrium
AV
Ventricle
1
2
3
4-11
12-13
14
100
0

Together these results demonstrated the ability of the noncontracting ventricle of 3-OST-7 morphants to release calcium from the sarcoplasmic reticulum and to re-uptake it at the end of the cycle. Particularly this indicates ryanodine receptors that are important in calcium cycling are functional in 3-OST-7 morphants. In addition, the calcium waves that were visualized by these imaging techniques (Supplemental Movies 2.5 through 2.8) indicated that the gap junctions that allow normal conduction to occur were also intact.

3-OST-7 is required for myofibrillogenesis and sarcomere assembly

The previous observations that action potentials and calcium transients were normally generated in 3-OST-7 morphants that had noncontracting ventricles illustrated the uncoupling of contraction from excitation. Moreover, this indicates defective contraction in 3-OST-7 morphants might be due to defects in the myocardial contractile apparatus, which is the direct target of calcium ions released from the sarcoplasmic reticulum during electrical excitation of the heart. To determine whether noncontraction of 3-OST-7 morphant ventricle is due to aberrant sarcomeres, we used immunohistochemistry to visualize proteins comprising the sarcomeric structure of the heart. Using MF20 and phalloidin to stain sarcomeric myosin and the actin filaments, respectively, we found that these filaments were disorganized in 3-OST-7 morphant hearts (Figure 2.5B and 2.5D) compared to the orderly arrays in hearts of control embryos (Figure 2.5A and 2.5C). Only ventricular myosin appeared to be disrupted; myosin filaments appeared to be normally organized in the atrium of 3-OST-7 morphants (Figure 2.5B). Furthermore, atrial myosin stained by S46 antibody was normal in both control embryos and 3-OST-7 morphants (data not shown). Cardiac troponin T and

Figure 2.5. Knockdown of 3-OST-7 disrupts sarcomere organization. Whole mount immunohistochemistry (IHC) was performed on fixed 48 hpf control (injected with control 3-OST-3Z MO) or 3-OST-7 morphant embryos to detect cardiac sarcomere proteins (n=30 for each group). The heart was then dissected out of the embryo, mounted on cover slips and imaged using a confocal microscope (thus, the dorso-ventral orientation of the mounted hearts was random). IHC using anti-myosin (MF20) and phalloidin revealed myosin and actin filaments were disorganized in ventricles of 3-OST-7 morphants (B and D) compared with control (A and C). IHC using anti-cardiac troponin T (Tnnt2) antibody and anti-tropomyosin (Tpm) antibody revealed levels of these proteins are greatly reduced in 3-OST-7 morphants (F and H) compared to control (E and G) embryos. At, atrium; V, ventricle.

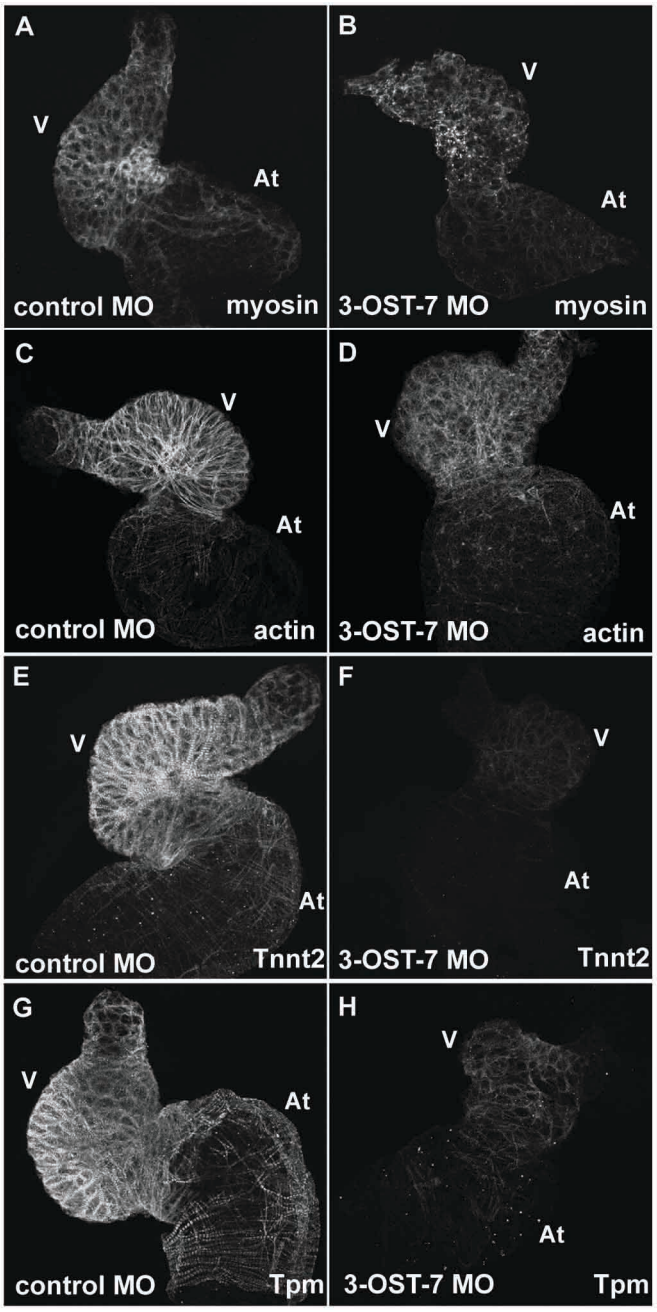
A
V
At
control MO
myosin
B
V
At
3-OST-7 MO
myosin
C
V
At
control MO
actin
D
V
At
3-OST-7 MO
actin
E
V
At
control MO
Tnnt2
F
V
At
3-OST-7 MO
Tnnt2
G
V
At
control MO
Tpm
H
V
At
3-OST-7 MO
Tpm

tropomyosin were also noticeably decreased in 3-OST-7 morphant hearts (Figure 2.5F and 2.5H) compared to control embryo hearts (Figure 2.5E and 2.5G). Together these results suggest the noncontraction of the ventricle in 3-OST-7 morphants is correlated with reduced levels and disorganization of sarcomere proteins.

3-OST-7 regulates transcription of tpm4

Strikingly, cardiac troponin T (*tnnt2*) and tropomyosin4 (*tpm4*) zebrafish mutants (Sehnert et al., 2002; Zhao et al., 2008) share similar phenotypes with the 3-OST-7 morphants. Both these mutants and 3-OST-7 morphants have noncontractile hearts and disorganized sarcomeres. Since it appears that 3-OST-7 regulates cardiac troponin T (Tnnt2) and tropomyosin (Tpm) protein levels (Figure 2.5F and 2.5H), we next addressed whether this regulation occurs at the transcriptional level for either of these sarcomeric genes. In situ analysis for *tnnt2* expression at 20 hpf, 24 hpf, and 48 hpf in morphants (Figure 2.6B, 2.6F, and 2.6J) revealed that *tnnt2* transcript levels were similar to control (Figure 2.6A, 2.6E, and 2.6I). In contrast transcript levels of *tpm4*, were reduced in 3-OST-7 morphants (Figure 2.6D, 2.6H, and 2.6L) compared to control embryos (Figure 2.6C, 2.6G, and 2.6K). Interestingly, we also found that *tpm4* mRNA levels were downregulated in 3-OST-7 morphant hearts in a microarray analysis comparing wild-type and 3-OST-7 morphant hearts at 48 hpf (data not shown).

Tpm4 is required for 3-OST-7 dependent ventricular contraction

The previous experiments demonstrated that 3-OST-7 is necessary for transcription of *tpm4*, which then ensures there would be normal levels of Tpm4 and presumably other sarcomeric proteins as well, such as Tnnt2. We next wanted to determine whether 3-OST-7 dependent transcription of *tpm4* is required for ventricular

Figure 2.6. 3-OST-7 controls expression of *tpm4*. *In situ* analysis for *tnnt2* showed comparable transcript levels and patterns of expression for 3-OST-7 morphants (B, F, and J) and control (injected with control 3-OST-5 MO) embryos (A, E, and I) at 20 hpf (A and B), 24 hpf (E and F), and 48 hpf (I and J). In contrast *tpm4* transcripts were decreased in 3-OST-7 morphants (D, H, and L) compared to control embryos (C, G, and K) at 20 hpf (C and D) and 24 hpf (G and H). Reduction is especially pronounced at 48 hpf (K and L). A through D are dorsal views with anterior on top; E to L are ventral views with anterior on top; n=40 for each group.

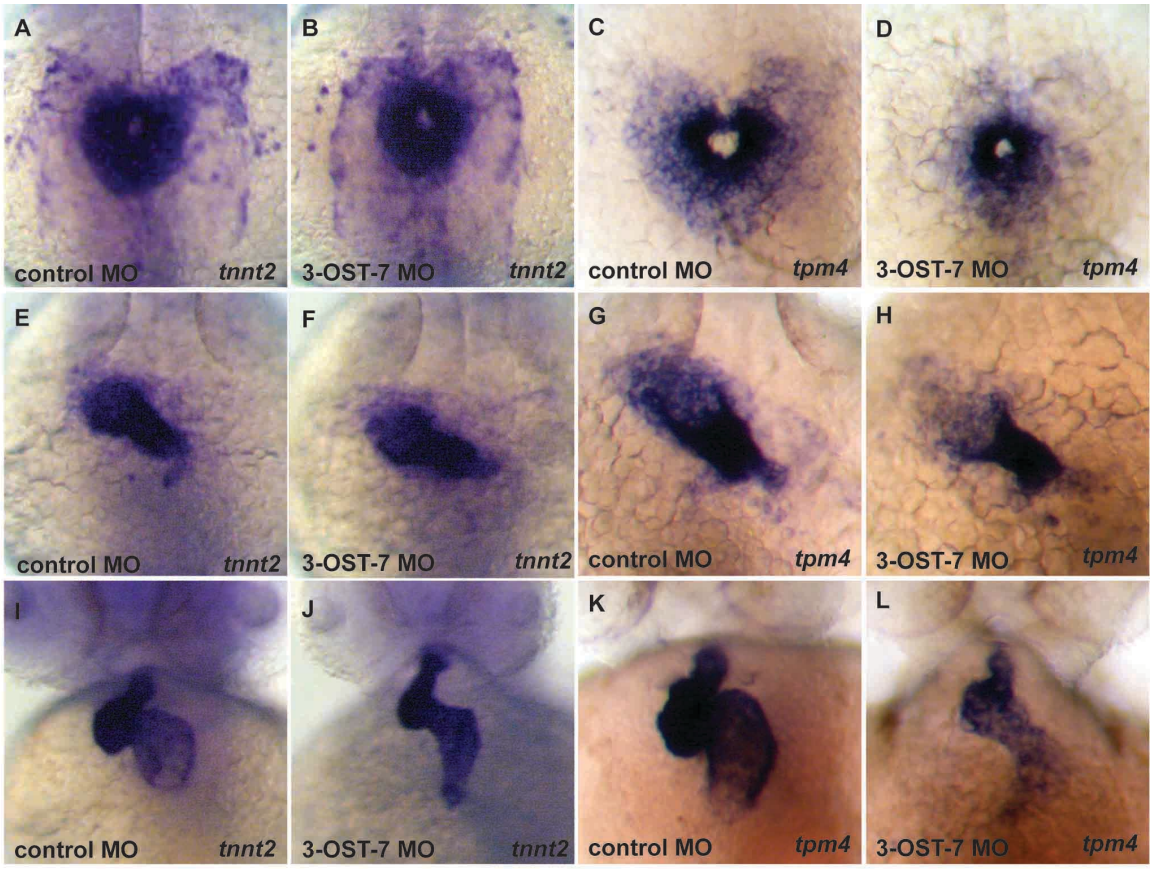
A
control MO
tnnt2
B
3-OST-7 MO
tnnt2
C
control MO
tpm4
D
3-OST-7 MO
tpm4
E
control MO
tnnt2
F
3-OST-7 MO
tnnt2
G
control MO
tpm4
H
3-OST-7 MO
tpm4
I
control MO
tnnt2
J
3-OST-7 MO
tnnt2
K
control MO
tpm4
L
3-OST-7 MO
tpm4

contraction. To examine this, we overexpressed *tpm4* by injection of *tpm4* RNA. Overexpression of *tpm4* RNA in control embryos had no perceived gross morphological effect, nor did it alter cardiac function (Figure 2.7). Strikingly, overexpression of *tpm4* RNA in 3-OST-7 morphants rescued ventricular noncontraction (Figure 2.7), demonstrating that *tpm4* is required for regulation of ventricular contraction by 3-OST-7.

Discussion

The significance of heparan sulfate proteoglycans (HSPGs) in developmental biology came about from genetic screens in invertebrates aimed at isolating patterning defects (Herman and Horvitz, 1999; Bulik et al., 2000; Duncan et al., 2001; Filmus and Selleck, 2001). Since then, most of the genes coding for the HSPG core proteins and the biosynthetic enzymes that build and modify the GAG chains have been identified (Cadwallader and Yost, 2006a, b, 2007). Strikingly, the GAG-chain modifying enzymes are encoded by multiple family members, but very few have been assayed for function.

In this study we demonstrate that one of the enzymes that places a rare 3-O-sulfation on the GAG chains, 3-OST-7, has a novel and highly specific function in cardiac development. In 3-OST-7 knockdown zebrafish, early cardiac cell specification, patterning, and cardiac tube looping are relatively normal, and atrium contraction is normal. In contrast, ventricle contraction is aberrant. By several methods, this ventricular noncontraction does not appear to be due to cellular electrophysiological defects. Strikingly, 3-OST-7 is required for the transcription and accumulation of *tpm4* mRNA in the ventricle, which then ensures that normal levels of Tpm4 protein are present. Tpm4 appears to be a lynchpin in sarcomere assembly and stabilization, because overexpression of Tpm4 protein by *tpm4* mRNA injection rescues the levels of other

Figure 2.7. Overexpression of *tpm4* rescues the noncontracting ventricle phenotype in 3-OST-7 morphant embryos. Overexpression of *tpm4* in control embryos did not alter cardiac function. Strikingly, overexpression in 3-OST-7 morphants rescued ventricular noncontraction ($P<3.0\text{x}10^{-3}$ for 3-OST-7 MO and 3-OST-7 MO + *tpm4* RNA).

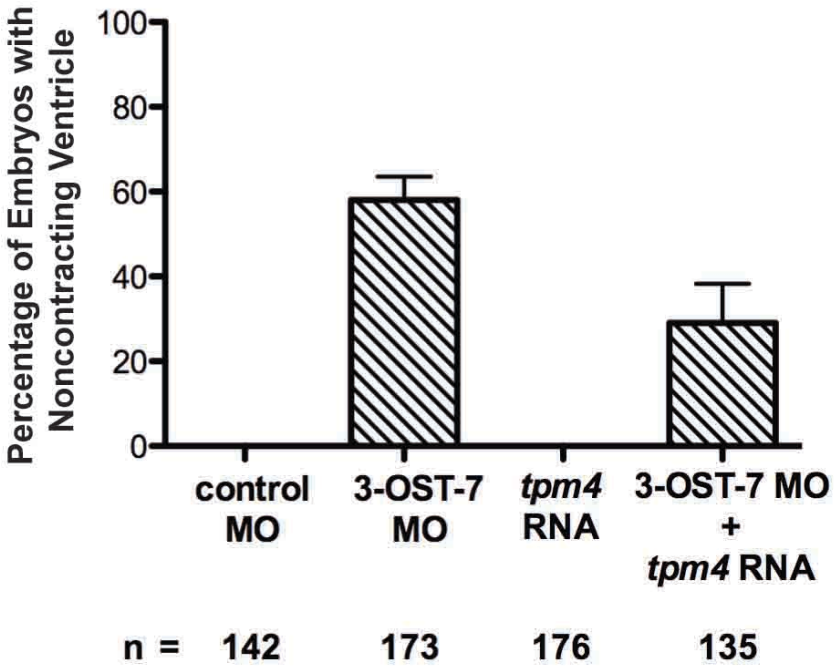
Percentage of Embryos with Noncontracting Ventricle
100
80
60
40
20
0
control MO
3-OST-7 MO
tpm4 RNA
3-OST-7 MO + tpm4 RNA
n = 142 173 176 135

sarcomeric proteins, rescues sarcomere structure, and rescues the ventricular contraction defect in 3-OST-7 morphants (Figure 2.8). Thus, knockdown of 3-OST-7 uncouples contraction from the normally functioning excitation cycle by perturbing *tpm4* transcription, leading to defective myofibrillogenesis. This places the 3-OST-7-dependent 3-O-sulfation of extracellular GAG chains as the first member of an otherwise unknown signaling pathway that is upstream of *tpm4* transcription and coordinated sarcomere assembly (Figure 2.8).

What is striking about the knockdown of 3-OST-7 is that the phenotype is only 50-60% penetrant, raising the possibility that another member of the 3-OST family can partially compensate for reduction of 3-OST-7. We have explored this possibility by knocking down several other members of the 3-OST family, and found that only one other member, 3-OST-1, the closest relative of 3-OST-7, has a similar cardiac phenotype as knockdown of 3-OST-7, with similar penetrance (data not shown). Furthermore, double knockdown of 3-OST-7 and 3-OST-1 increased penetrance of the cardiac ventricular phenotype (data not shown), arguing that these two 3-OSTs are partially functionally redundant. However, knockdown of 3-OST-1 has a more severe effect on the heart, including defects in atrial contraction as well.

Another intriguing aspect of the 3-OST-7 knockdown is the organ-specific phenotype, despite ubiquitous 3-OST-7 expression in early development (Cadwallader and Yost, 2006b). The cardiac ventricular contraction defect in 3-OST-7 morphants could be rescued by ubiquitous transgenic expression of 3-OST-7 protein (with a modified construct that could not bind morpholino), indicating that the cardiac contraction phenotype is specific for 3-OST-7 function, not an off-target effect of morpholinos. In

Figure 2.8. Model for role of 3-O-sulfation catalyzed by 3-OST-7 in cardiac development. Under normal conditions, specific 3-O-sulfation patterns interact with unidentified molecule and activate a signaling pathway that turns on transcription of *tpm4*. Tpm4 then stabilizes the sarcomere and ensures proper contraction. Knocking down 3-OST-7 results in loss of 3-O-sulfation and reduced levels of *tpm4* transcripts and Tpm4 proteins, which then disrupt sarcomere assembly, leading to defective contraction.

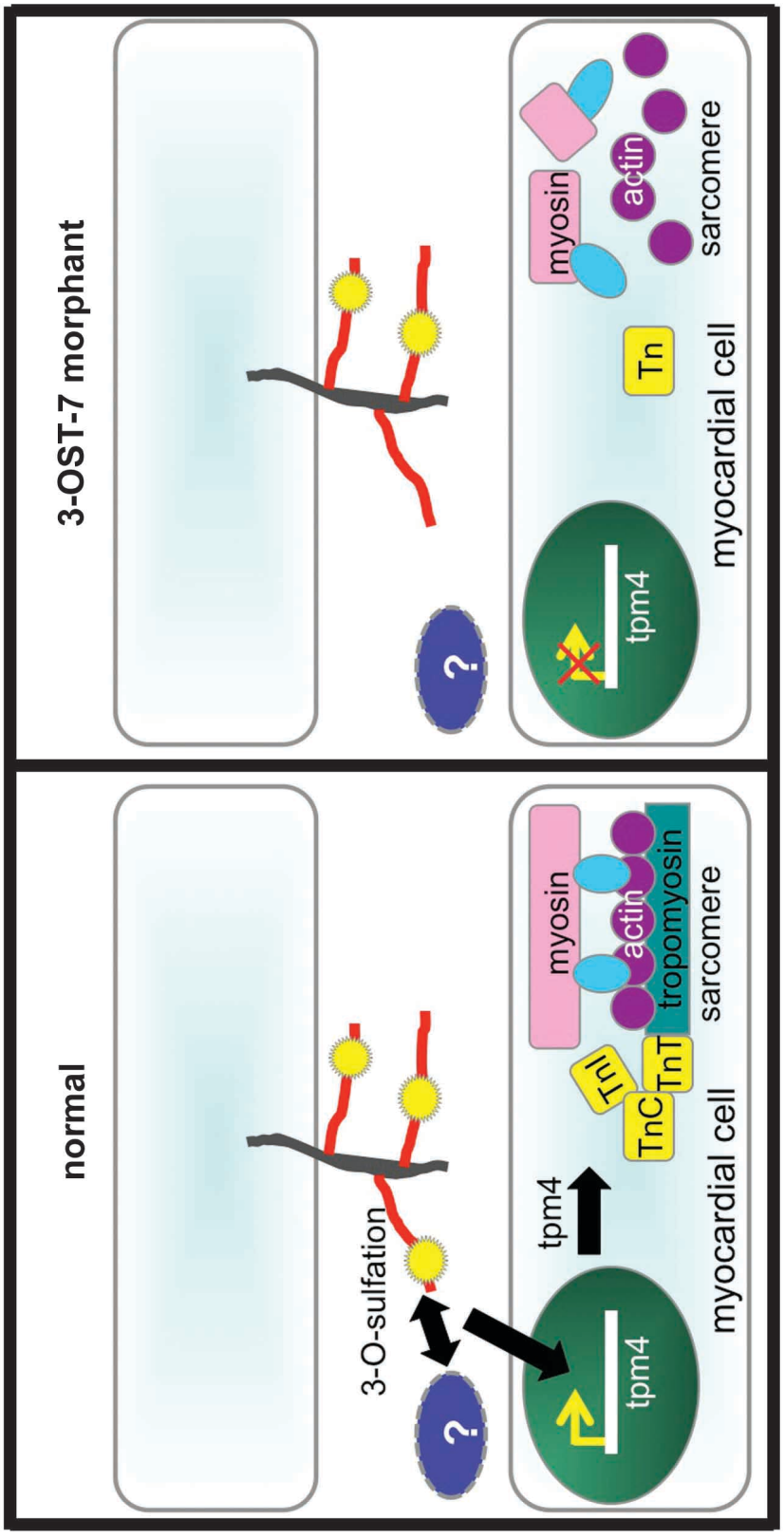
normal
3-O-sulfation
?
tpm4
myosin
actin
TnI
TnC
TnT
tropomyosin
sarcomere
myocardial cell
3-OST-7 morphant
?
tpm4
myosin
actin
Tn
sarcomere
myocardial cell

contrast, it is curious that the cardiac phenotype is not rescued by a *cmlc2*-driven transgene that expresses just in cardiomyocytes. While it is possible that 3-OST-7 expression is required in some other neighboring tissue, and not in *cmlc2*-positive cardiomyocytes (thus, Figure 2.8 proposes a cell-cell communication to regulate *tmp4* transcription), we cannot exclude the possibility that 3-OST-7 is also required in cardiomyocytes but that the timing or strength of *cmlc2* transgene expression is insufficient to rescue the knockdown. Nonetheless, ubiquitous expression of *tpm4*, by mRNA injection into one-cell embryos, does not by itself alter cardiac function, but is able to rescue the 3-OST-7 knockdown cardiac contraction phenotype.

We propose that 3-OST-7-dependent 3-O-sulfation of GAG chains on cell surface or extracellular HSPGs is required for activation of an unknown cell-cell signaling pathway that regulates transcription of a lynchpin sarcomere protein, Tpm4 (Figure 2.8). Other components that are upstream of Tpm4 regulation are unknown. It is possible that the Notch pathway participates, since sulfation by 3-OST-B, one of two 3-OSTs in *Drosophila*, is implicated to interact with the Notch signaling pathway (Kamimura et al., 2004). However, known Notch mutants (Holley et al., 2000) or pharmacological inhibition of the Notch pathway do not have ventricular contraction defects similar to 3-OST-7 knockdown (data not shown). Another pathway, FGF signaling, was considered because FGF signaling has been shown to be dependent on HSPGs for receptor-ligand complex formation in vitro (Yayon et al., 1991; Pellegrini et al., 2000; Schlessinger et al., 2000; Lin, 2004). However, known FGF pathway mutants (Reifers et al., 2000; Marques and Yelon, 2009) or morphants (Neugebauer et al., 2009) have not been reported to have specific ventricular contraction defects, and pharmacological inhibition does not result in

similar defects (Neugebauer et al., 2009). It is possible that the 3-OST-7 specific GAG modification is required to modulate the convergence of multiple signaling pathways to regulate transcription of *tpm4*, sarcomere assembly and ventricular contraction.

Zebrafish is an outstanding model organism to study the coordination of embryonic cardiac morphogenesis with physiological function. Our study demonstrates that 3-OST-7 is required for normal heart function, but is dispensable for specification of cardiac lineages and early formation of the heart. We anticipate that further investigation of this 3-OST-7 knockdown model will greatly improve our understanding of how specific modifications of HSPGs shape heart development and cardiac function. Exploring the effects of noncontraction on later steps of cardiac morphogenesis will also be instructive in assessing feedback loops between function and structure. Ultimately, defining the pathway that transmits the 3-OST-7-dependent sulfation signal to its demonstrated role in cardiac function will offer major insights as to how extracellular information is relayed to cellular behavior.

Materials and methods

Zebrafish strains and lines

Zebrafish were maintained under standard laboratory conditions at 28.5°C. In addition to Oregon AB wild-type, the following transgenic lines were used: *Tg(cmlc2:GFP)*(Huang et al., 2003), *Tg(fli1:EGFP)* (Lawson and Weinstein, 2002), *Tg(cmcl2:gCaMP)*^{s878} (Chi et al., 2008).

Morpholino and RNA injection

The following morpholino oligonucleotides and their corresponding concentrations were used: 3-OST-7 MO1 (translation-blocking MO with sequence 5'-

CACATAACTCAGAAGATTGGCCATG-3', 5.4 ng) and 3-OST-7 MO2 (splice-blocking MO with sequence 5'- CACATCTGGAAGACACAAGAGAGAG-3', 1.4 ng) to knockdown 3-OST-7; 3-OST-5 MO (5'-GTCCAGTCAGGTCAAGGGCAGCTCA-3', 2.7 ng) and 3-OST-3Z MO (5'-GTCCAGTCAGGTCAAGGGCAGCTCA-3', 5.4 ng), which targeted other 3-OSTs, as control. Embryos were injected at the 1-2 cell stage.

Transgenesis and rescue

The Tol2kit cloning system (Kwan et al., 2007) was used to generate *Tg(cmlc2:3-OST-7-IRES-EGFP)* and *Tg(β-actin:3-OST-7-IRES-EGFP)*. The middle entry vector encoding 3-OST-7 was generated using the pCS2-3-OST-7 expression vector as a source construct. It does not contain 3-OST-7 MO2 binding sequence so that 3-OST-7 MO2 would not inhibit transgenic expression of 3-OST-7. Multisite recombination reactions were performed as previously described (Kwan et al., 2007). Transposase RNA was synthesized using mMessage mMachine kit (Ambion). 25 pg of transposase RNA and 30 pg of *cmlc2:3-OST-7-IRES-EGFP* or 30 pg of *β-actin:3-OST-7-IRES-EGFP* plasmid DNA were injected into wild-type AB fish at the one-cell stage. Potential transgenic founders (F_0) were identified by scoring for GFP expression in hearts (*cmlc2:3-OST-7-IRES-EGFP*) or ubiquitous GFP expression (*β-actin:3-OST-7-IRES-EGFP).* Potential F_0s were then crossed to wild-type AB fish to check for GFP expression. Those that gave GFP-positive transgenic embryos were subsequently used for rescue experiments where 1.4 ng of 3-OST-7 MO2 was injected into embryos from F_0 x AB matings. At 48 hpf, embryos were sorted by GFP fluorescence, then scored for ventricular noncontraction.

tpm4 RNA was synthesized using the mMessage mMachine kit (Ambion) from the linearized pXT7-tpm4-tv1 expression vector. The vector was a generous gift from

Anming Meng (Zhao et al., 2008). 175 pg of RNA was co-injected with 5.4 ng of 3-OST-7 MO1 at the one-cell stage.

In situ hybridization

Digoxigenin-labeled antisense riboprobes were synthesized using Digoxigenin RNA Labeling Kit (Roche). cDNA plasmids encoding *hand2*, *nkx2.5*, *cmlc2*, *amhc* (a gift from Priya Choudhry), *vmhc*, *tnnt2*, and *tpm4* (a gift from Anming Meng) were used. *In situ* hybridizations were performed as previously described (Essner et al., 2000), with anti-digoxigenin antibody incubation carried out using a Biolane HTI machine. Embryos were cleared in 70% glycerol and photographed with a Nikon SMZ1000 camera. Digital images were processed with Adobe Photoshop CS4.

Action potential recordings

Forty-eight hpf larvae were dechorionated and anesthetized with 0.02% tricaine for 1 to 2 minutes. The heart was dissected from the thorax *en bloc* by using fine forceps and transferred to the recording chamber. Only spontaneously beating whole hearts were studied. All experiments were performed at 22^{o}C to 24^{o}C. The recording chamber was perfused with external control solution containing (in mmol/L) NaCl 140, KCl 4, $CaCl_2$ 1.8, $MgCl_2$ 1, glucose 10, and HEPES 10 (pH 7.4). Suction pipettes were made from borosilicate capillary tubes and fire-polished to obtain resistances of 6-9 MΩ when filled with solution containing (in mmol/L) KCl 120, EGTA 5, K_2ATP 5, $MgCl_2$ 5, and HEPES 10 (pH 7.2). The pipette was positioned adjacent to the heart and a seal was formed by application of minimal suction. Using this technique, stable spontaneous APs were recordable for up to 3 hours.

Calcium transient recordings and optical mapping

Two methods were used to observe calcium transients. In the first method, Ca^{2+} transients were recorded in spontaneously beating explanted hearts at 48 hpf using fluo-4 (Molecular Probes) loading and high-speed confocal scanning. Hearts were first incubated in the external control solution containing 10 μM fluo 4-AM and 0.35 mM probenicid at 25°C for 2 min. Probenicid was included to help retard fluo-4 loss from the cells. The heart was then continuously bathed in the external control solution containing probenicid. High speed scanning at 63 frames/sec was achieved with a confocal microscope (Zeiss 5-Live, excitation 489 nm, emission LP 505, 40x oil). Fluorescent signals (F) were normalized to baseline values (F_o). The maximum Ca^{2+} transient amplitude (F_{Max}/ F_o) was determined by averaging the peak amplitude of three consecutive transient signals. The decay of the calcium transient was determined by a monoexponential fit of the decaying signal and averaging value of three consecutive transient signals.

The other method utilized optical mapping in 3-OST-7 MO-injected and control MO-injected transgenic *Tg(cmlc2:gCaMP)*^{s878} embryos as previously described (Chi et al., 2008).

Immunohistochemistry

Immunohistochemistry using the primary antibodies MF20 (Developmental Studies Hybridoma Bank, 1:10), CT3 (Developmental Studies Hybridoma Bank, 1:10) and CH1 (Developmental Studies Hybridoma Bank, 1:10) was performed as described previously (Neugebauer et al., 2009). Secondary antibody, either donkey anti-mouse Alexa Fluor 488 (Molecular Probes) or goat anti-mouse Alexa Fluor 488 (Molecular Probes), was used in 1:100 dilution. Images were acquired using an Olympus Fluoview

FV300 laser scanning confocal microscope. Digital images were processed with Adobe Photoshop CS4.

Statistics

For rescue experiments in *Tg*(*β-actin:3-OST-7-IRES-EGFP)* or *Tg*(*β-actin:3-OST-7-IRES-EGFP)*, two-way ANOVA was performed using GraphPad Prism (version 5.00 for Mac GraphPad Software). For calcium transient amplitude and decay measurements, and *tpm4* RNA rescue experiments, Student's *t*-test was performed.

Supplemental movies

Movie 2.1. Movie shows lateral view of beating heart in control (uninjected, wild-type) *Tg(cmlc2:gfp)* embryo at 48 hpf. Ventricle is left, atrium is right.

Movie 2.2. Movie shows lateral view of impaired ventricular contraction in 3-OST-7 morphant *Tg(cmlc2:gfp)* embryo at 48 hpf. Ventricle is left, atrium is right.

Movie 2.3. Movie shows normal circulation in the trunk of control (uninjected, wild-type embryo.

Movie 2.4. Movie shows poor circulation in the trunk of 3-OST-7 morphant embryo.

Movie 2.5. Movie shows calcium waves in explanted heart stained with Fluo-4 of control (injected with control 3-OST-5 MO) embryo. Ventricle is right, atrium is left.

Movie 2.6. Movie shows calcium waves in explanted heart stained with Fluo-4 of 3-OST-7 morphant embryo. Ventricle is right, atrium is left.

Movie 2.7. Movie shows calcium activation and progression of conduction in control (injected with control 3-OST-3Z MO) *Tg(cmlc2:gCaMP)*^{s878} embryo. Atrium is on top.

Movie 2.8. Movie shows calcium activation and progression of conduction in 3-OST-7 morphant *Tg(cmlc2:gCaMP)*^{s878} embryo. Atrium is slightly out of focus on top.

References

Bers DM (2002) Cardiac excitation-contraction coupling. Nature 415:198-205.

Bulik DA, Wei G, Toyoda H, Kinoshita-Toyoda A, Waldrip WR, Esko JD, Robbins PW, Selleck SB (2000) sqv-3, -7, and -8, a set of genes affecting morphogenesis in Caenorhabditis elegans, encode enzymes required for glycosaminoglycan biosynthesis. Proc Natl Acad Sci U S A 97:10838-10843.

Bulow HE, Hobert O (2006) The molecular diversity of glycosaminoglycans shapes animal development. Annu Rev Cell Dev Biol 22:375-407.

Cadwallader AB, Yost HJ (2006a) Combinatorial expression patterns of heparan sulfate sulfotransferases in zebrafish: II. The 6-O-sulfotransferase family. Dev Dyn 235:3432-3437.

Cadwallader AB, Yost HJ (2006b) Combinatorial expression patterns of heparan sulfate sulfotransferases in zebrafish: I. The 3-O-sulfotransferase family. Dev Dyn 235:3423-3431.

Cadwallader AB, Yost HJ (2007) Combinatorial expression patterns of heparan sulfate sulfotransferases in zebrafish: III. 2-O-sulfotransferase and C5-epimerases. Dev Dyn 236:581-586.

Chi NC, Shaw RM, Jungblut B, Huisken J, Ferrer T, Arnaout R, Scott I, Beis D, Xiao T, Baier H, Jan LY, Tristani-Firouzi M, Stainier DY (2008) Genetic and physiologic dissection of the vertebrate cardiac conduction system. PLoS Biol 6:e109.

Duncan G, McCormick C, Tufaro F (2001) The link between heparan sulfate and hereditary bone disease: finding a function for the EXT family of putative tumor suppressor proteins. J Clin Invest 108:511-516.

Esko JD, Selleck SB (2002) Order out of chaos: assembly of ligand binding sites in heparan sulfate. Annu Rev Biochem 71:435-471.

Essner JJ, Branford WW, Zhang J, Yost HJ (2000) Mesendoderm and left-right brain, heart and gut development are differentially regulated by pitx2 isoforms. Development 127:1081-1093.

Evans SM, Yelon D, Conlon FL, Kirby ML (2010) Myocardial lineage development. Circ Res 107:1428-1444.

Filmus J, Selleck SB (2001) Glypicans: proteoglycans with a surprise. J Clin Invest 108:497-501.

Glickman NS, Yelon D (2002) Cardiac development in zebrafish: coordination of form and function. Semin Cell Dev Biol 13:507-513.

Hacker U, Nybakken K, Perrimon N (2005) Heparan sulphate proteoglycans: the sweet side of development. Nat Rev Mol Cell Biol 6:530-541.

Herman T, Horvitz HR (1999) Three proteins involved in Caenorhabditis elegans vulval invagination are similar to components of a glycosylation pathway. Proc Natl Acad Sci U S A 96:974-979.

Holley SA, Geisler R, Nusslein-Volhard C (2000) Control of her1 expression during zebrafish somitogenesis by a delta-dependent oscillator and an independent wave-front activity. Genes Dev 14:1678-1690.

Huang CJ, Tu CT, Hsiao CD, Hsieh FJ, Tsai HJ (2003) Germ-line transmission of a myocardium-specific GFP transgene reveals critical regulatory elements in the cardiac myosin light chain 2 promoter of zebrafish. Dev Dyn 228:30-40.

Kamimura K, Rhodes JM, Ueda R, McNeely M, Shukla D, Kimata K, Spear PG, Shworak NW, Nakato H (2004) Regulation of Notch signaling by Drosophila heparan sulfate 3-O sulfotransferase. J Cell Biol 166:1069-1079.

Kwan KM, Fujimoto E, Grabher C, Mangum BD, Hardy ME, Campbell DS, Parant JM, Yost HJ, Kanki JP, Chien CB (2007) The Tol2kit: a multisite gateway-based construction kit for Tol2 transposon transgenesis constructs. Dev Dyn 236:3088-3099.

Lamanna WC, Kalus I, Padva M, Baldwin RJ, Merry CL, Dierks T (2007) The heparanome--the enigma of encoding and decoding heparan sulfate sulfation. J Biotechnol 129:290-307.

Lawson ND, Weinstein BM (2002) In vivo imaging of embryonic vascular development using transgenic zebrafish. Dev Biol 248:307-318.

Lin X (2004) Functions of heparan sulfate proteoglycans in cell signaling during development. Development 131:6009-6021.

Marques SR, Yelon D (2009) Differential requirement for BMP signaling in atrial and ventricular lineages establishes cardiac chamber proportionality. Dev Biol 328:472-482.

Neugebauer JM, Amack JD, Peterson AG, Bisgrove BW, Yost HJ (2009) FGF signalling during embryo development regulates cilia length in diverse epithelia. Nature 458:651-654.

Noseda M, Peterkin T, Simoes FC, Patient R, Schneider MD (2011) Cardiopoietic factors: extracellular signals for cardiac lineage commitment. Circ Res 108:129-152.

Park PW, Reizes O, Bernfield M (2000) Cell surface heparan sulfate proteoglycans: selective regulators of ligand-receptor encounters. J Biol Chem 275:29923-29926.

Pellegrini L, Burke DF, von Delft F, Mulloy B, Blundell TL (2000) Crystal structure of fibroblast growth factor receptor ectodomain bound to ligand and heparin. Nature 407:1029-1034.

Reifers F, Walsh EC, Leger S, Stainier DY, Brand M (2000) Induction and differentiation of the zebrafish heart requires fibroblast growth factor 8 (fgf8/acerebellar). Development 127:225-235.

Schlessinger J, Plotnikov AN, Ibrahimi OA, Eliseenkova AV, Yeh BK, Yayon A, Linhardt RJ, Mohammadi M (2000) Crystal structure of a ternary FGF-FGFR-heparin complex reveals a dual role for heparin in FGFR binding and dimerization. Mol Cell 6:743-750.

Schoenebeck JJ, Keegan BR, Yelon D (2007) Vessel and blood specification override cardiac potential in anterior mesoderm. Dev Cell 13:254-267.

Sehnert AJ, Huq A, Weinstein BM, Walker C, Fishman M, Stainier DY (2002) Cardiac troponin T is essential in sarcomere assembly and cardiac contractility. Nat Genet 31:106-110.

Stainier DY (2001) Zebrafish genetics and vertebrate heart formation. Nat Rev Genet 2:39-48.

Stern MD (1992) Theory of excitation-contraction coupling in cardiac muscle. Biophys J 63:497-517.

Yayon A, Klagsbrun M, Esko JD, Leder P, Ornitz DM (1991) Cell surface, heparin-like molecules are required for binding of basic fibroblast growth factor to its high affinity receptor. Cell 64:841-848.

Yelon D, Horne SA, Stainier DY (1999) Restricted expression of cardiac myosin genes reveals regulated aspects of heart tube assembly in zebrafish. Dev Biol 214:23-37.

Zhao L, Zhao X, Tian T, Lu Q, Skrbo-Larssen N, Wu D, Kuang Z, Zheng X, Han Y, Yang S, Zhang C, Meng A (2008) Heart-specific isoform of tropomyosin4 is essential for heartbeat in zebrafish embryos. Cardiovasc Res 80:200-208.

CHAPTER 3

3-OST-7 REGULATES A FEEDBACK LOOP BETWEEN BMP SIGNALING AND CARDIOMYOCYTE CONTRACTION

Abstract

Cardiac function and circulation begin long before heart development is completed, making the heart an excellent system for studying the interrelationship between structure and function in development. In this study, we utilized the 3-OST-7 knockdown in zebrafish, which causes ventricular noncontraction, to demonstrate that contraction affects specific aspects of cardiac maturation, including the transition from an isometric cell shape to an elongated cell shape, and a feedback loop between *bmp4* expression and contractility. 3-OST-7 morphants had ectopic expression of *bmp4* in the ventricle, which also occurred in two distinct contraction defect models, knockdown of the potassium voltage-gated channel gene *kcnh2* (affected in Romano-Ward syndrome and long-QT syndrome) or knockdown of *tnnt2* (tropomyosin-binding cardiac troponin T type 2, affected in human cardiomyopathies). These results reveal a correlation between noncontraction and ectopic *bmp4* expression. Strikingly, cardiac contraction was rescued in 3-OST-7 morphants by the $bmp4^{st72}$ mutation, demonstrating that a feedback loop controlled by 3-OST-7 exists between myocardial contraction and *bmp4* expression. Together, these findings illustrate an intriguing interrelationship between cardiac structure and function that is modulated by 3-OST-7 and BMP4.

Introduction

Vertebrate heart development requires an accurate integration of patterning and morphogenetic events leading eventually to the formation of a fully functional heart. It initiates with the specification of the different tissue lineages that will compose the mature heart, followed by an intricate set of differentiation events that will transform the early heart field into a mature, beating organ. This transformation is defined by the subspecialization of regions of the primitive heart tube to acquire characteristics of chamber myocardium or maintenance of some characteristics of the tube in nonchamber myocardium. These complex events are orchestrated by a network of signals and transcription factors that could act differentially depending upon specific spatiotemporal cues. Among the important players are major signaling pathways such as BMP signaling and Wnt signaling, which set the early stages of differentiation (Shi et al., 2000; Walters et al., 2001; Yang et al., 2006; Mandel et al., 2010), and the T-box (Tbx) family of transcription factors that confer chamber or nonchamber identity to the primitive heart tube (Hoogaars et al., 2007).

Ultimately, generation of a beating heart is the goal of these processes. For the heart to contract, contractile proteins must be produced and assembled in units called sarcomeres and their contraction must be coupled to the electrical activation of the heart. The heart starts beating during the late stages of heart tube formation, and through its mechanical action, affects subsequent differentiation steps as shown in studies correlating defective morphogenesis with abnormal function (Rottbauer et al., 2001; Xu et al., 2002; Berdougo et al., 2003; Huang et al., 2003). This makes the heart an excellent model system to study the relationship between form and function and to elucidate the

intermediate steps and signaling pathways involved. In this study, we used the 3-O-sulfotransferase-7 (3-OST-7) morpholino (MO) knockdown model in zebrafish, in which contraction of the ventricle is uncoupled from excitation due to defects in myofibrillogenesis.

3-OST-7 is a member of a family of enzymes responsible for 3-O-sulfation in zebrafish. This type of modification is associated with the glycosaminoglycan (GAG) chains present on heparan sulfate proteoglycans (HSPGs), biologically important molecules whose functions are due, in part, to these GAG chains (Esko and Selleck, 2002). The location of HSPGs, on the cell surface or in the extracellular matrix, and their structural heterogeneity place them at a unique advantage to influence signaling pathways and cell-cell or cell-matrix interactions (Esko and Lindahl, 2001). This versatility has been demonstrated in various animal models where genes involved in biosynthesis and modification of HSPGs have been knocked out or knocked down (Bulow and Hobert, 2006).

Knocking down 3-OST-7 in zebrafish through the use of MO resulted in a noncontracting ventricle phenotype, which can be rescued by ubiquitous overexpression of 3-OST-7 in a transgenic (*Tg(β-actin:3-OST-7)*) zebrafish embryo. We have also previously demonstrated that 3-OST-7 regulates transcription of a sarcomere gene, *tpm4*, and shown that the noncontracting ventricle phenotype can be rescued by overexpression of *tpm4* RNA. In this study, we examine the relationship between contraction and morphogenesis, and elucidate the signaling pathways and gene regulation involved.

Results

3-OST-7 is required for normal ventricular cardiomyocyte morphology

Marker analysis and visualization of the heart tube indicate early processes involved in heart development including heart field specification, cardiac fusion, and heart tube formation were normal (data not shown). This would also argue that the 3-OST-7 morphant ventricle achieved an early stage of differentiation, but then retained the characteristics of the primitive heart tube and did not proceed to further mature. We wanted to determine whether morphological aspects of differentiation were aberrant in 3-OST-7 morphant ventricles.

Normally, ventricular precursors have an isometric cell shape at 24 hours postfertilization (hpf), which becomes elongated at 48 hpf (Auman et al., 2007). To determine whether this change in cell morphology occurs in 3-OST-7 morphants we performed whole-mount immunohistochemistry (IHC) to fluorescently label the cell membrane and compare cell areas using morphometric analysis. We used anti-β-catenin antibody to outline the cells (Figure 3.1A and 3.1D) of 48 hpf *Tg(cmlc2-DsRed-nuc)* embryos (Mably et al., 2003). This transgenic line ensured we were comparing myocardial cells (Figure 3.1B and 3.1E). We observed that ventricular cells in control embryos had elongated morphologies (Figure 3.1A and 3.1C). In contrast 3-OST-7 morphant ventricular cardiomyocytes retained an isometric morphology at 48 hpf (Figure 3.1D and 3.1F). Using morphometric analysis to quantitate the observed morphological difference between control and 3-OST-7 morphant embryos, we found that the

Figure 3.1. Ventricular cardiomyocytes in 3-OST-7 morphants fail to transition from isometric to elongated cell shape. Whole mount immunohistochemistry (IHC) was performed on fixed 48 hpf control embryos (injected with control 3-OST-3Z MO) and 3-OST-7 morphants to compare cell morphologies and areas in *Tg(cmlc2-DsRed-nuc)* zebrafish (Mably et al., 2003). IHC using anti-β-catenin (A and D) and anti-DsRed (B and E, *cmlc2-nuc* stands for nuclear expression of *cmlc2-DsRed*) allowed for delineation of cardiac cell membranes (red dotted outlines) and measurement of their areas. C and F are merged images of anti-β-catenin (green) and DsRed (red) staining. (G) Graph showing comparison of cell surface area (μm^2) measurements for control and 3-OST-7 morphants. Surface area of ventricular cardiomyocytes in 3-OST-7 morphants was significantly smaller compared to control ($P<1.0x10^{-4}$) (H) Graph showing comparison of circularity measurements for control and 3-OST-7 morphants. A value of 1 corresponds to a perfect circle. Ventricular cardiomyocytes in 3-OST-7 morphants were significantly rounder than those in control ($P<4.0x10^{-3}$). For the surface area and circularity measurements, five cells were chosen from each of 10 embryos in each injection group, and cell tracings, surface area measurements, and shape assessments were done using ImageJ software (NIH).

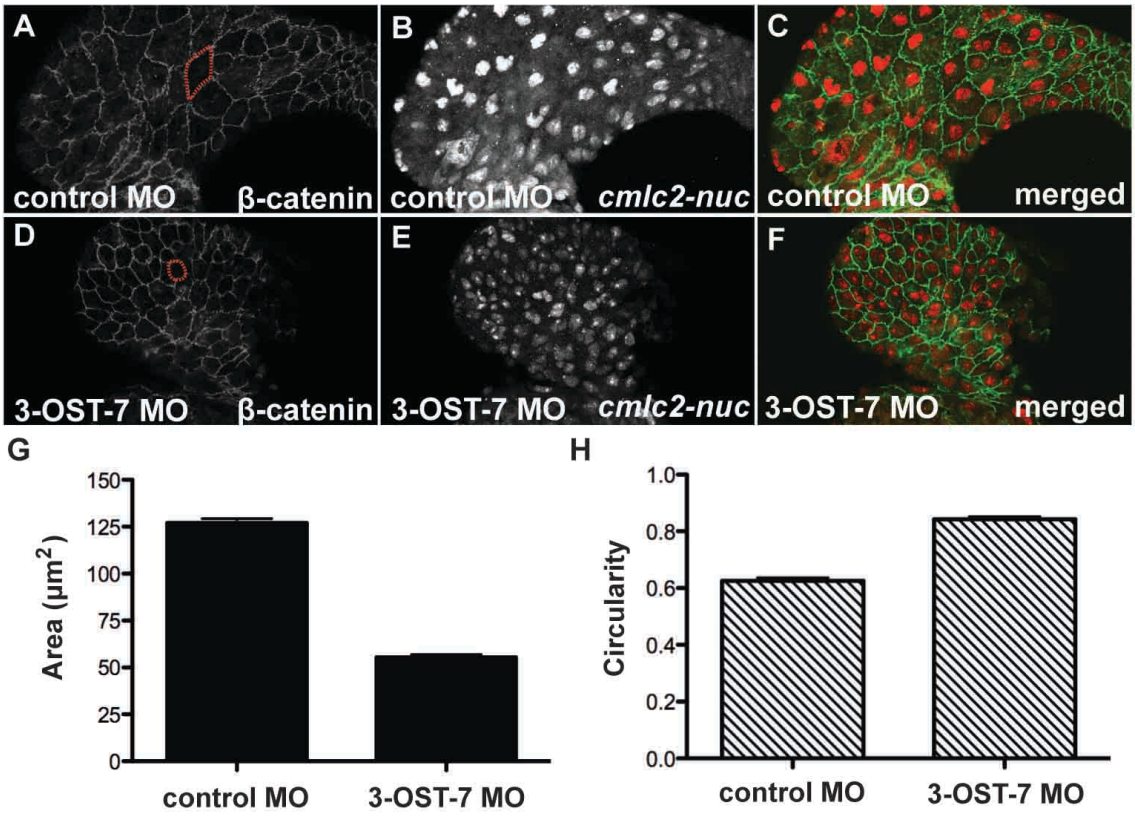
A
control MO
β-catenin
B
control MO
cmlc2-nuc
C
control MO
merged
D
3-OST-7 MO
β-catenin
E
3-OST-7 MO
cmlc2-nuc
F
3-OST-7 MO
merged
G
Area (μm²)
150
125
100
75
50
25
0
control MO
3-OST-7 MO
H
Circularity
1.0
0.8
0.6
0.4
0.2
0.0
control MO
3-OST-7 MO

ventricular cardiomyocyte surface area was significantly smaller in 3-OST-7 morphants (Figure 3.1G). Furthermore, shape assessments determined these cells were rounded compared to the elongated shape of control ventricular myocytes (Figure 3.1H). These results demonstrate that ventricular cardiomyocytes in 3-OST-7 morphants do not undergo the cell morphological change that is one of the hallmarks of ventricular maturation.

3-OST-7-controlled ventricular contraction is not regulated by FGF and Notch signaling pathways

To elucidate the pathways involved in 3-OST-7 regulation of ventricular maturation and contraction, we started with two major developmental signaling pathways as candidates, FGF and Notch signaling. FGF was the first growth factor shown to require GAG chains for receptor-ligand complex formation and *in vivo* studies have highlighted the role of GAG chains in FGF signaling (Yayon et al., 1991; Pellegrini et al., 2000; Schlessinger et al., 2000; Lin, 2004). If loss of 3-O-sulfation caused by knockdown of 3-OST-7 perturbs FGF signaling, loss of FGF signaling should mimic the noncontracting ventricle phenotype of 3-OST-7 morphants. To test this, we knocked down FGF receptor 1 (FGFR1) using morpholino in zebrafish embryos. Knocking down FGFR1 resulted in ventricles that were smaller but still retained their ability to contract (Figure 3.2A). This is consistent with reports wherein abolishing FGF signaling either by using the zebrafish *fgf8/ace* mutant or treatment with the FGFR inhibitor SU5402 also resulted in small hearts with particularly notable reductions of the ventricle (Reifers et al., 2000; Marques et al., 2008). The distinct phenotype suggest that the FGF signaling pathway is not downstream of 3-OST-7-catalyzed 3-O-sulfation.

In *Drosophila*, 3-O-sulfation by 3-OST-B has been implicated to play an important role in the Notch pathway (Kamimura et al., 2004). More importantly, *deltaD*, a Notch ligand, was one of the most downregulated genes in microarray analysis comparing control embryo hearts and 3-OST-7 morphant hearts at 48 hpf (data not shown). To determine whether 3-OST-7 regulates ventricular contraction by way of the Notch signaling pathway, we assessed whether the noncontracting ventricle phenotype is recapitulated in *deltaD/aei*^{AG49} mutant embryos (Holley et al., 2000). Embryos carrying a homozygous mutation in the *deltaD* gene were identified by misformed somites posterior to the ninth somite (Holley et al., 2000) and separated from wild-type or heterozygous siblings at 18 hpf. The hearts were then scored for ventricular contraction at 48 hpf. The hearts of *deltaD/aei*^{AG49} mutants contracted similar to hearts of siblings (n=34 with perturbed somite patterning (mutants); n=94 rest of the clutch (wild-type siblings)). Since DeltaD is one of four Delta ligands in zebrafish, it is possible that other Delta ligands might be compensating for loss of DeltaD in *deltaD/aei*^{AG49} mutants and masking effects on ventricular contraction. To circumvent this, we used DAPT, a γ-secretase inhibitor of all Notch signaling. Treatment from 5 hpf, the time when cells are fated to become myocytes (Stainier et al., 1993), to 48 hpf, the time when the 3-OST-7 noncontracting ventricle phenotype is clearly manifest, did not result in ventricular noncontraction (Figure 3.2B). Similar observations were made when the treatment was started later, either at 15 hpf or 24 hpf (Figure 3.2B). Together these results demonstrate the Notch pathway does not mediate 3-OST-7-regulated ventricular contraction.

Figure 3.2. Disrupting the FGF and Notch signaling pathways do not phenocopy the noncontracting ventricle phenotype of 3-OST-7 knockdown. (A) Table showing percentage of normal contraction and small ventricles in control (uninjected) embryos, embryos injected with 4 ng *fgfr1* MO1, and embryos injected with 8 ng *fgfr1* MO2 at 48 hpf. Ventricular contraction appeared normal in all groups. (B) Timeline showing the time and duration of 75 μM DAPT treatment and table showing percentage of embryos with normal contraction. Control embryos were treated with 0.3%(v/v) DMSO. Ventricular contraction appeared normal in all treatments. To ensure the DAPT was working, embryos treated with DAPT starting at 5 hpf were observed at 18 hpf for somite defects. No somite disruption was observed in corresponding DMSO treatments.

A

	n	% Normal Contraction	% Small Ventricle
control	158	100	0
fgfr1 MO1	163	100	64.9
fgfr1 MO2	141	100	34.6

B

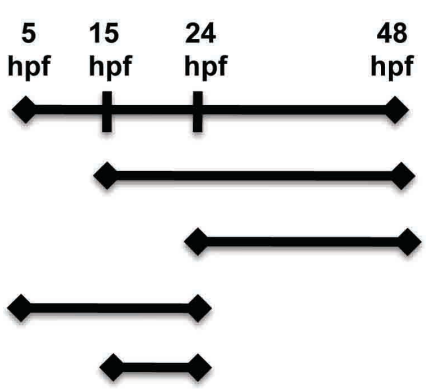

DMSO		DAPT	
n	% Normal Contraction	n	% Normal Contraction
30	100	30	100
28	100	30	100
30	100	25	100
25	100	27	100
29	100	28	100

3-OST-7 is required for normal region-specific gene expression of bmp4 and versican

In addition to the cardiomyocyte shape change, the cardiac maturation program also involves genes that become differentially expressed in a spatial and temporal manner. *Bmp4*, *versican*, and *notch1b* are progressively restricted during heart development. At 24 hpf, all three genes are expressed along the antero-posterior length of the heart, and are subsequently restricted to the atrioventricular (AV) canal by 48 hpf (Westin and Lardelli, 1997; Walsh and Stainier, 2001; Beis et al., 2005) and excluded from expression in the maturing ventricle. In contrast in 3-OST-7 morphants, *bmp4* and *versican* were ectopically expressed in ventricle at 48 hpf (Figure 3.3B and Figure 3.3D), whereas both are restricted to the AV canal and excluded from ventricle in control embryos (Figure 3.3A and 3.3C). *Bmp4* and *versican* remained ectopically expressed in ventricle cardiomyocytes at 3 days postfertilization (data not shown). In contrast to *bmp4* and *versican*, *notch1B* was expressed solely in the AV canal for 3-OST-7 morphants (Figure 3.3F) similar to control embryos (Figure 3.3E), and *tie2* expression, assessed in *Tg(tie2:EGFP)* embryos, was expressed normally in the AV canal in both control and 3-OST-7 morphant embryos (Figure 3.3G and 3.3H), suggesting that the failure of *bmp4* and *versican* to become AV canal-restricted was not merely due to developmental delay. Together these results indicate the differentiation program does not occur completely in 3-OST-7 morphants. Moreover, the observation that *notch1B* expression was normal in 3-OST-7 morphants is consistent with our finding that the Notch pathway is not involved in 3-OST-7-mediated ventricular contraction.

Figure 3.3. 3-OST-7 regulates expression of myocardial genes *bmp4* and *versican* at 48 hpf. *In situ* hybridization for *bmp4* (A and B), *versican* (C and D), and *notch1B* (E and F) shows *bmp4* and *versican* were ectopically expressed in ventricular myocardium of 3-OST-7 morphants (B and D), whereas *notch1B* was restricted to AV endocardium (F). Control group (A, C and E) were injected with control 3-OST-5 MO. *Tie2* expression, assessed in *Tg(tie2:EGFP)* embryos, was normally expressed in 3-OST-7 morphant AV endocardium (G). Control (F) was uninjected embryo. V, ventricle; At, atrium; red arrows point to AV.

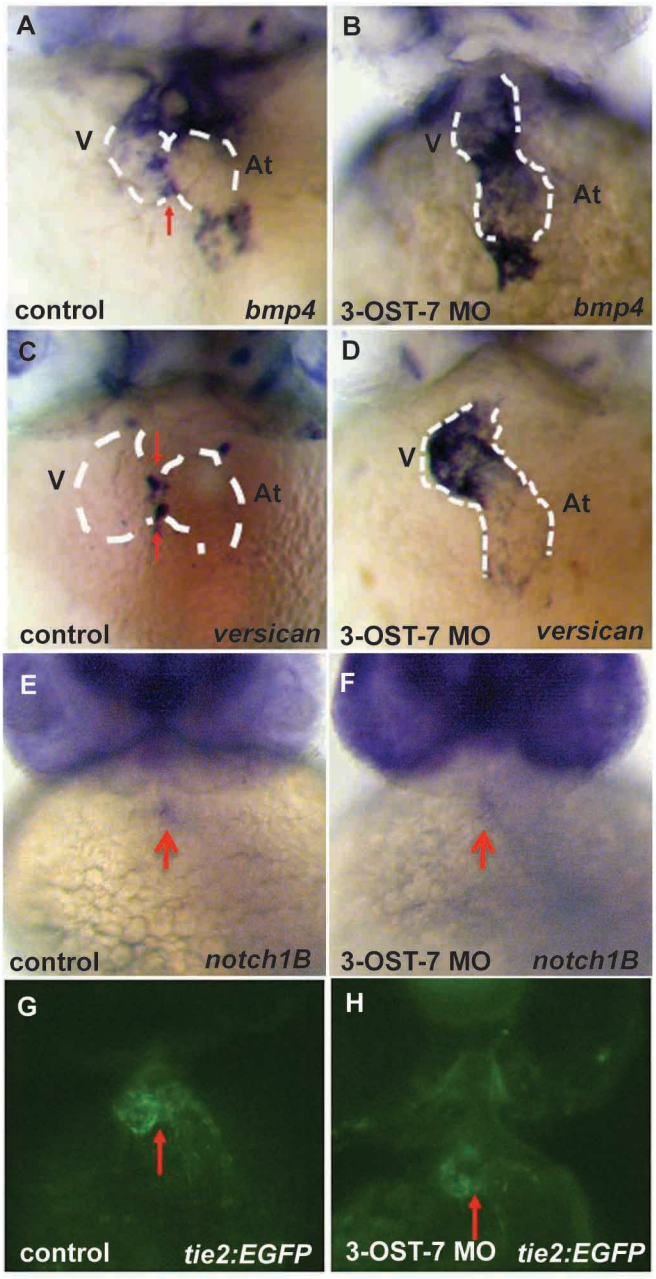
A
V
At
control
bmp4
B
V
At
3-OST-7 MO
bmp4
C
V
At
control
versican
D
V
At
3-OST-7 MO
versican
E
control
notch1B
F
3-OST-7 MO
notch1B
G
control
tie2:EGFP
H
3-OST-7 MO
tie2:EGFP

Myocardial contraction excludes bmp4 from the ventricle

The observations that *bmp4* and *versican* were ectopically expressed in the ventricular myocardium, while *notch1B* and *tie2* were normally expressed in the endocardium at the AV canal, suggest that 3-OST-7 morphants have a maturation defect that is specific to ventricular myocardium. Moreover, these observations suggest ectopic *bmp4* expression in the ventricular myocardium could be a result of ventricular noncontraction. To determine whether ectopic expression of *bmp4* and *versican* is due to noncontraction, we examined two other contractility morphants and assessed whether *bmp4* expression in these mutants is similar to that of 3-OST-7 morphants. We used morpholinos against the potassium channel gene *kcnh2* and sarcomeric protein cardiac troponin T gene *tnnt2*. *Kcnh2* and *tnnt2* mutants both have "silent" (i.e., noncontracting) hearts and morpholino knockdown of these genes phenocopy the mutant phenotypes (Sehnert et al., 2002; Arnaout et al., 2007).

We examined *bmp4* expression in the *kcnh2* and *tnnt2* morphants and classified it to be one of three: normal, AV-restricted expression (AV only, green bar in Figure 3.4B), ectopically expressed in ventricle (AV + V, red bar in Figure 3.4B), and ectopically expressed in atrium and ventricle (AV + V + At, blue bar in Figure 3.4B). Strikingly, *bmp4* was ectopically expressed in *kcnh2* and *tnnt2* morphants (Figure 3.4B). Only 23.4% and 5.7% of embryos had normal AV-restricted expression with injection of *kcnh2* and *tnnt2* MO, respectively (green bars in Figure 3.4B), whereas a large fraction of embryos, 76.6% and 94.3% for *kcnh2* and *tnnt2* morphants, respectively, had ectopic expression (red and blue bars in Figure 3.4B).

Moreover, the fraction of embryos with ectopic *bmp4* expression was larger in *kcnh2* and *tnnt2* morphants than in 3-OST-7 morphants. Interestingly, the percentage of ectopic *bmp4* expression correlated with percentage of noncontraction (Figure 3.4A and 3.4B). For example, knockdown of 3-OST-7 resulted in 56.9% of embryos having ventricular noncontraction (Figure 3.4A) and 48.8% had ectopic *bmp4* expression (red and blue bars, Figure 3.4B), the least noncontraction and ectopic *bmp4* expression fractions observed among the three MO knockdowns. In contrast, knockdown of *tnnt2* resulted in 99.4% of embryos with noncontraction (Figure 3.4A), the highest noncontraction fraction among the three knockdowns, which correlated with the highest fraction of ectopic *bmp4* expression (red and blue bars, Figure 3.4B). These results suggest contraction is required for restricting *bmp4* expression to the AV canal and excluding it from the ventricle and atrium.

Next we asked whether this apparent effect of contraction on *bmp4* expression is affecting the transition of ventricular cardiomyocytes from isometric morphology to elongated morphology. We utilized the same technique we used for tracing ventricular cardiomyocyte outlines in 3-OST-7 morphants (Figure 3.1A and 3.1D) and used morphometric analysis to compare surface areas and shapes. The surface area of ventricular cardiomyocytes was significantly reduced in *kcnh2* and *tnnt2* morphants, but not to the extent it was observed in 3-OST-7 morphants (Figure 3.4C). Notably, ventricular cardiomyocytes were elongated in *kcnh2* and *tnnt2* morphants (Figure 3.4D). This suggests that the cardiomyocyte morphological defect observed in 3-OST-7 morphants is not a secondary effect that could be generalized for noncontraction resulting from other types of perturbations.

Figure 3.4. Contraction is correlated with ectopic *bmp4* expression, whereas cell morphological change is dependent on regulation of contraction by 3-OST-7. (A) Graph comparing the penetrance of noncontraction phenotype with 3-OST-7, *kcnh2*, and *tnnt2* MO injections. (B) Graph comparing patterns of *bmp4* expression at 48 hpf between control embryos (injected with 3-OST-5 MO), 3-OST-7 morphants, *kchn2* morphants, and *tnnt2* morphants. Instead of normal expression at the AV canal (AV only), loss of contraction leads to ectopic *bmp4* expression in the ventricle (AV + V) or throughout the heart (AV + V + At) in 3-OST-7, *kcnh2* and *tnnt2* morphants. (C) Graph comparing cell surface area (μm^2) measurements for control embryos (injected with 3-OST-3Z MO), 3-OST-7 morphants, *kcnh2* morphants, and *tnnt2* morphants. Surface areas were significantly smaller in 3-OST-7, *kcnh2*, and *tnnt2* morphants than in control embryos ($P<1.0x10^{-4}$ for control and 3-OST-7, $P<3.0x10^{-2}$ for control and *kcnh2*, $P<1.0x10^{-2}$ for control and *tnnt2*). (D) Graph showing comparison of circularity measurements for control (injected with 3-OST-3Z MO), 3-OST-7 morphants, *kcnh2*, and *tnnt2* morphants. Ventricular cardiomyocytes in 3-OST-7 morphants were more rounded than those in control embryos ($P<4.0x10^{-3}$), whereas ventricular cardiomyocytes in *kcnh2* and *tnnt2* morphants were as elongated as those in control ($P<6.2x10^{-2}$ for control and *kcnh2*, $P<5.8x10^{-2}$ for control and *tnnt2*).

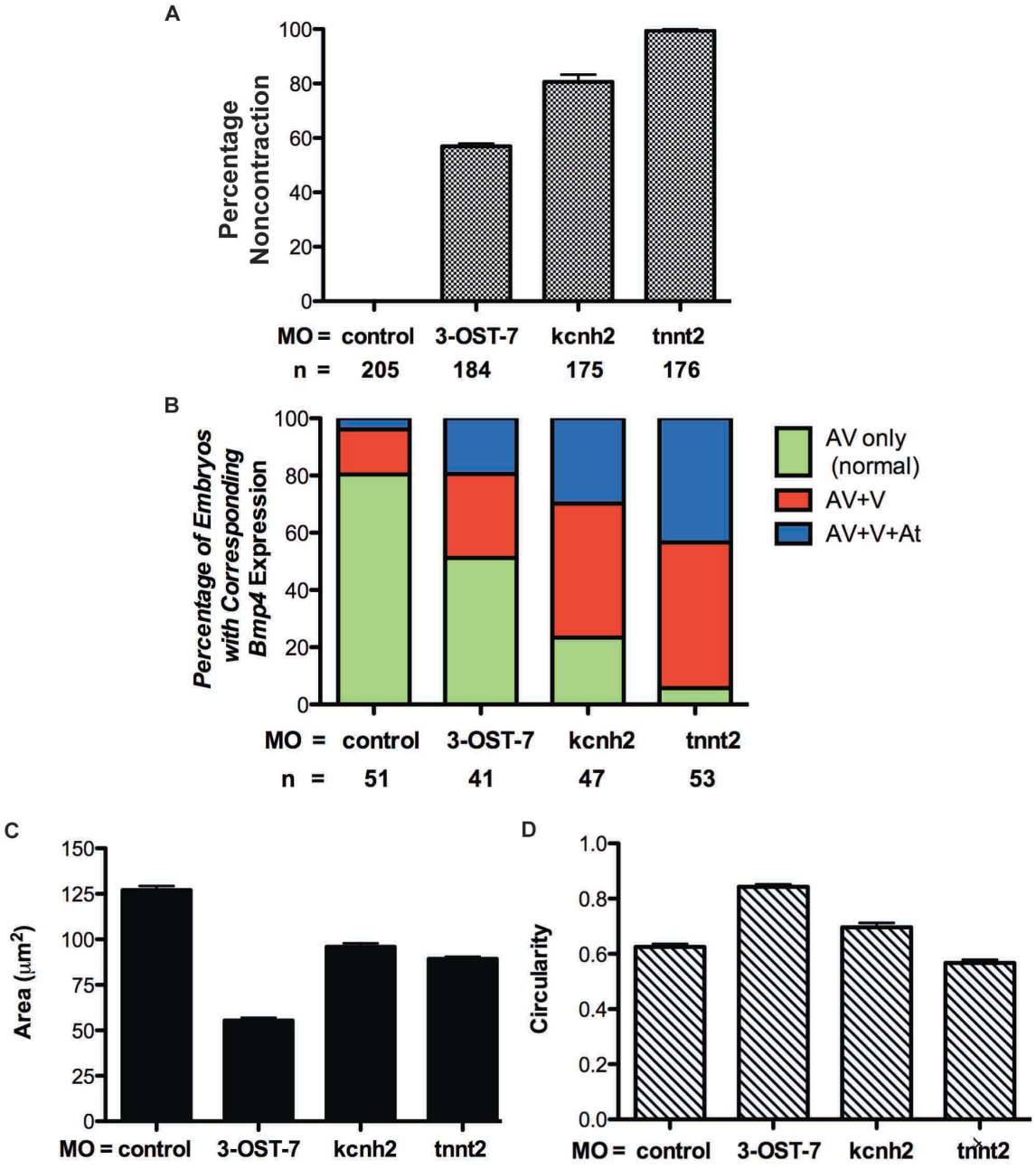
A
Percentage Noncontraction
100
80
60
40
20
0
MO = control 3-OST-7 kcnh2 tnnt2
n = 205 184 175 176
B
Percentage of Embryos with Corresponding Bmp4 Expression
100
80
60
40
20
0
AV only (normal)
AV+V
AV+V+At
MO = control 3-OST-7 kcnh2 tnnt2
n = 51 41 47 53
C
Area (μm²)
150
125
100
75
50
25
0
MO = control 3-OST-7 kcnh2 tnnt2
D
Circularity
1.0
0.8
0.6
0.4
0.2
0.0
MO = control 3-OST-7 kcnh2 tnnt2

Ectopic bmp4 expression in 3-OST-7 morphants is not due to general patterning defect

The restriction of *bmp4* in the AV canal is part of a more comprehensive patterning of myocardial cells that have undergone the early stages of differentiation into either chamber myocardium (atrium or ventricle) or nonchamber myocardium (sinus venosus, AV canal, and outflow tract) (Harvey et al., 2009; Evans et al., 2010). To determine whether ectopic *bmp4* expression in 3-OST-7 morphants is a result of defects in patterning the chamber and nonchamber myocardium, we performed *in situ* hybridization for *tbx2* (*tbx2b* in zebrafish) and *anf* in 48 hpf control embryos and 3-OST-7 morphants. *Tbx2b* is normally expressed in the AV canal (nonchamber myocardium) at 48 hpf (Chi et al., 2008), and we observed a similar pattern of expression in both control embryos and 3-OST-7 morphants (Figure 3.5A and 3.5B). Similarly, *anf*, which is normally expressed in atrium and ventricle (chamber myocardium) at 48 hpf (Figure 3.5C), had a similar pattern of expression in 3-OST-7 morphants (Figure 3.5D). Together these results suggest that ectopic *bmp4* expression in the ventricle of 3-OST-7 morphants is not due to a general defect in patterning chamber and nonchamber myocardium.

3-OST-7-mediated regulation of bmp4 expression feeds back to contraction

Expression of *bmp4* has been used extensively as a marker for normal AV patterning in zebrafish, with ectopic expression correlated with defects in valve formation. Whether this ectopic expression leads to other defects in those regions where it is ectopically expressed has not been elucidated. We hypothesize that the ectopic expression of *bmp4* in the ventricle exacerbates the noncontracting phenotype. To test

Figure 3.5. Chamber (working) and nonchamber (nonworking) myocardium appear delineated in 3-OST-7 morphants. *In situ* hybridization for *tbx2b* (A and B), a nonchamber myocardium-specific marker, and *anf* (C and D), a chamber myocardium-specific marker, suggests delineation between chamber and nonchamber myocardium occurs normally in 3-OST-7 morphants. Control (A and B) are embryos injected with control 3-OST-5 MO. Red arrows point to AV.

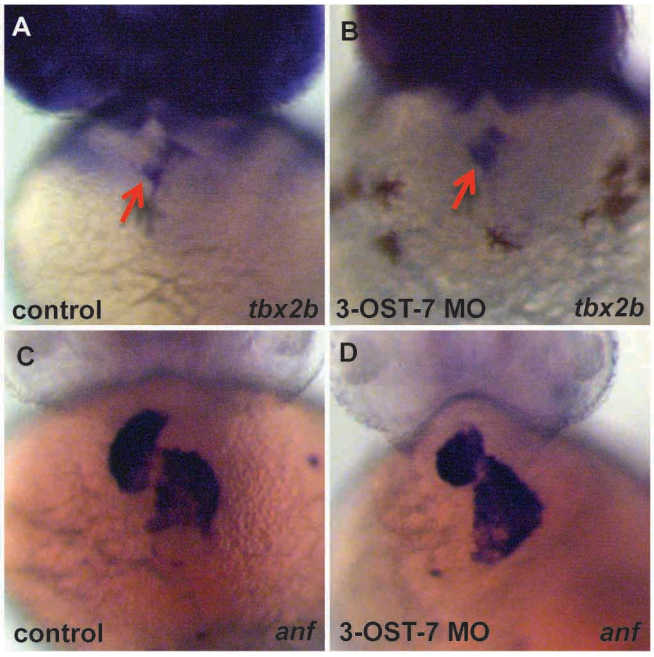
A
control
tbx2b
B
3-OST-7 MO
tbx2b
C
control
anf
D
3-OST-7 MO
anf

this, we utilized the zebrafish *bmp4*^{st72} mutant (Stickney et al., 2007) and asked whether reduction of *bmp4* will rescue the noncontracting ventricle phenotype caused by knockdown of 3-OST-7. We injected 3-OST-7 MO into embryos from crosses between *bmp4*^{st72}/+ heterozygotes, with uninjected embryos from the same genetic crosses serving as control. The embryos were then segregated by heart phenotype: normal hearts, AV defects, or noncontracting ventricles at 48 hpf. The AV defect is characterized by an obscure boundary between atrium and ventricle (data not shown). The embryos were then individually genotyped. In uninjected embryos (n=163), the noncontracting ventricle phenotype was not observed for *bmp4*^{st72} mutants. The percentage of embryos with the noncontracting ventricle phenotype, observed at 62.5% of 3-OST-7 MO injected wild-type siblings (+/+), was reduced for 3-OST-7 MO injected *bmp4*^{st72} mutants (-/-), with only 10% of these mutants having a noncontracting ventricle (n=55 for 3-OST-7 MO injected embryos) (Figure 3.6). Genomic DNA of the injected *bmp4*^{st72} mutants were sequenced to determine whether each contains the correct target site for the 3-OST-7 MO. This is to confirm that the 3-OST-7 MO sequence was targeting 3-OST-7 in the *bmp4*^{st72} mutant line.

This demonstrates that ectopic expression of *bmp4* exacerbates the noncontracting ventricle phenotype of 3-OST-7 morphants, because elimination of *bmp4* expression through the *bmp4*^{st72} mutant resulted in the rescue of the noncontracting ventricle phenotype. Furthermore this demonstrates that 3-OST-7 and *bmp4* act in a feedback loop to control contraction.

Figure 3.6. Ventricular noncontraction is rescued in 3-OST-7 morphants by *bmp4*^{st72} mutation. Graphs depicting the percentage of embryos with noncontracting ventricle (red) or defective AV (green) in three genotypic classes of uninjected *bmp4*^{st72} embryos (A) or *bmp4*^{st72} embryos injected with 3-OST-7 MO (B).

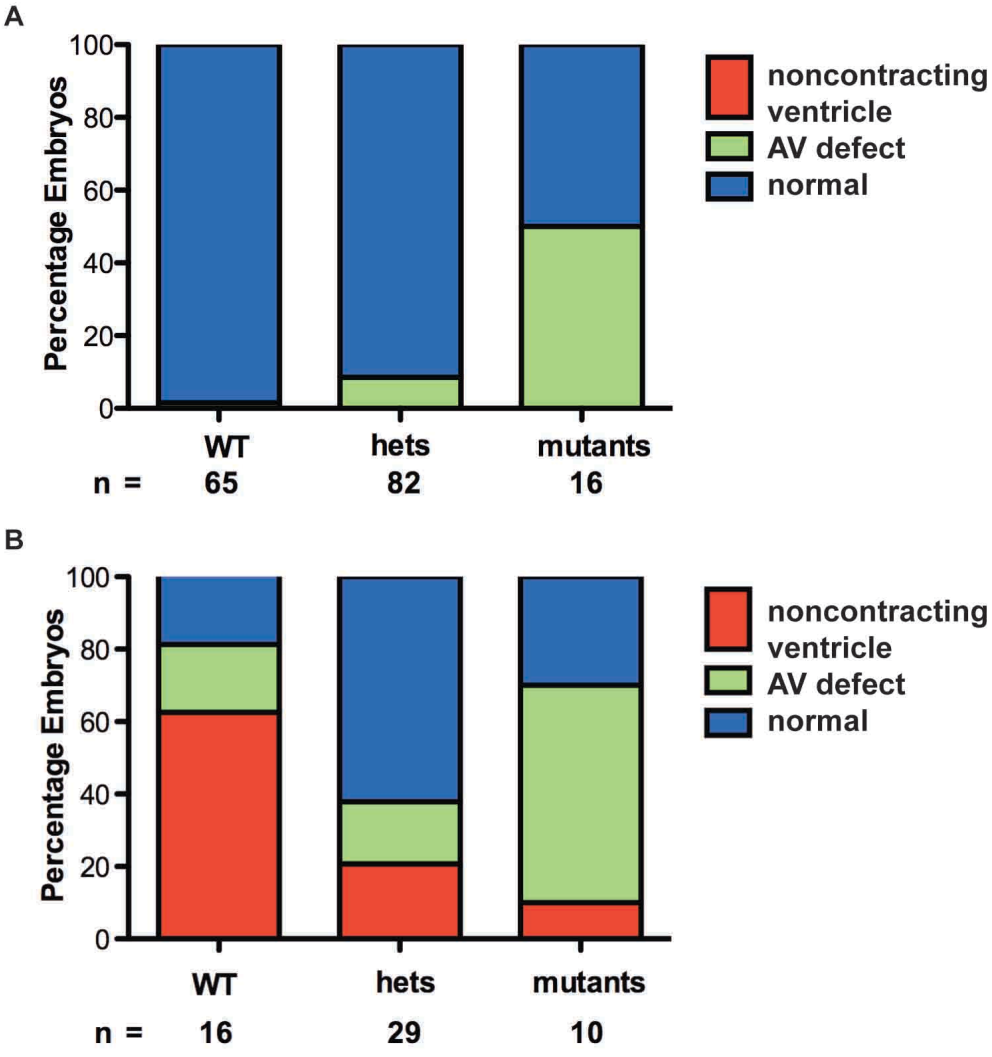
A
Percentage Embryos
100
80
60
40
20
0
WT
hets
mutants
n = 65 82 16
noncontracting ventricle
AV defect
normal
B
Percentage Embryos
100
80
60
40
20
0
WT
hets
mutants
n = 16 29 10
noncontracting ventricle
AV defect
normal

Discussion

The function of the heart begins before it has completed developing, prompting the question of whether contraction is required for the differentiation events that occur after the heart starts beating. Although the relationship of structure and function in heart development has been addressed in previous studies (Bartman et al., 2004; Bartman and Hove, 2005; Auman et al., 2007), questions remain as to which pathways mediate this relationship.

In this study we demonstrate that contractility has a novel and highly specific function in gene expression. Knockdown of 3-OST-7 eliminates ventricular contraction and results in failure of ventricular cardiomyocytes to transition from isometric to elongated cell shape and in ectopic expression of *bmp4* and *versican* in the ventricle. By in situ hybridization for markers of the endocardium, chamber myocardium, and nonchamber myocardium, the defects in morphogenesis and gene expression do not appear to be due to a general defect in differentiation. Strikingly, knockdowns of two other genes, *kcnh2* and *tnnt2*, which eliminate contraction by distinct pathways, also resulted in ectopic expression of *bmp4* in the ventricle. Notably, percentage of embryos with ectopic expression of *bmp4* is correlated with the penetrance of noncontraction with the MO knockdown. To illustrate, knockdown of 3-OST-7 MO had the least percentage of embryos with ectopic *bmp4* expression and also had the least penetrant noncontraction phenotype, whereas knockdown of *tnnt2* had the most fraction of embryos with ectopic *bmp4* expression and also the most penetrant noncontraction phenotype. Our findings support the concept that myocardial function affects differentiation processes occurring after the first heartbeat, and demonstrate that defective contraction alters *bmp4*

expression. In contrast to the correlation between contraction and *bmp4* expression, the transition from isometric to elongated cell shape appears relatively normal in *kcnh2* and *tnnt2* morphants, suggesting that this cellular phenotype could not be generalized for all contractility defects, but is a result of noncontraction specific to 3-OST-7 knockdown.

Another intriguing question is whether ectopic *bmp4* expression in the ventricle leads to defects specific to the ventricle. Strikingly, ventricular noncontraction is rescued in 3-OST-7 morphants by *bmp4*^{st72} mutation, suggesting 3-OST-7 and *bmp4* are in a feedback loop that controls contraction. We hypothesize 3-OST-7 might function in two modes in this pathway (Figure 3.7). First, 3-OST-7 allows for normal ventricular contraction (1 in Figure 3.7), which then inhibits expression of *bmp4* in the ventricle (2 in Figure 3.7). This is supported by our data on the tight correlation between three distinct pathways that eliminate contraction (knockdown of 3-OST-7, *kcnh2* or *tnnt2*) and corresponding ectopic *bmp4* expression in the ventricle. Second, HSPGs that are specifically modified by 3-OST-7 might inhibit expression of *bmp4* in the ventricle (3 in Figure 3.7) and this inhibition blocks the inhibitory action of *bmp4* on contraction (4 in Figure 3.7), allowing normal ventricular contraction. Intersection of these two modes of action result in a feedback loop, which is supported by our finding that 3-OST-7 knockdown-induced ventricular noncontraction can be rescued back to normal contraction in *bmp4*^{st72} mutants.

Determining the signaling pathways that mediate 3-OST-7 regulation of *bmp4* expression and contraction would help us elucidate this feedback loop. Our findings that perturbation of the FGF and Notch signaling pathways did not result in ventricular noncontraction, along with previous studies (Reifers et al., 2000; Marques et al., 2008),

Figure 3.7. Model for role of 3-OST-7 in regulating a feedback loop between *bmp4* expression and cardiomyocyte contraction. For the heart to develop normally, 3-OST-7 functions in a feedback loop to regulate both contraction and inhibition of *bmp4* expression in the ventricle.

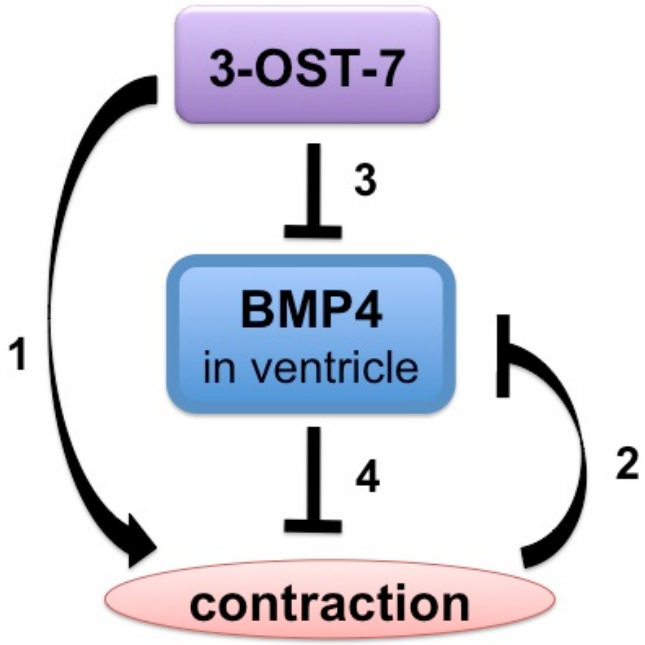
3-OST-7
3
BMP4
in ventricle
1
2
4
contraction

suggest that these pathways are not involved in 3-OST-7 regulation of contraction. However, we could not discount the possibility that 3-OST-7 modulates multiple pathways to regulate contraction. With regards to 3-OST-7 regulation of *bmp4* expression, it could occur directly by interaction of 3-OST-7-modified HSPGs with Bmp4 protein, leading to *bmp4* feedback inhibition of its own expression and inhibiting subsequent expression of *bmp4* in ventricle. In this direct interaction scenario, knockdown of 3-OST-7 leads to derepression of Bmp4 functions, including suppression of contraction and hyperactivation of BMP signaling, and leads to increased *bmp4* expression. The alternative possibility is that 3-OST-7 is modulating another pathway that inhibits *bmp4* expression in the ventricle.

The zebrafish 3-OST-7 knockdown model provides an outstanding system to study the relationship between structure and function. Our study demonstrates that 3-OST-7 regulates both contraction and *bmp4* expression in the ventricle, and that each of these processes are tightly linked in a feedback loop. We anticipate that further investigation of this feedback loop between contraction and gene expression, with regards to defining the pathways that mediate them, will greatly improve our understanding of cardiac morphogenesis and will continue to highlight the significance of 3-O-sulfation in cardiac development, physiology and function.

Materials and methods

Zebrafish strains and lines

Zebrafish were maintained under standard laboratory conditions at 28.5°C. In addition to Oregon AB wild-type, the transgenic *Tg(cmlc2-DsRed-nuc)* (Mably et al., 2003) and *Tg(tie2:EGFP)* zebrafish (Motoike et al., 2000), and the zebrafish

deltaD/aei^{AG49} (Holley et al., 2000) and *bmp4*^{st72} (Stickney et al., 2007) mutants were used.

Morpholino injection

Antisense MOs were obtained from Gene Tools, LLC. The following morpholino oligonucleotides and their corresponding concentrations were used: translation-blocking 3-OST-7 MO (5'-CACATAACTCAGAAGATTGGCCATG-3', 5.4 ng); translation-blocking 3-carboxyfluorescein-labelled FGFR1 MO1 (5'-GCAGCAGCGTGGTCTTCATTATCAT-3', 4 ng) (Scholpp et al., 2004; Thummel et al., 2006) and translation-blocking 3-carboxyfluorescein-labelled FGFR1 MO2 (5'-CAAAGATCCTCTACATCTGAACTCC-3', 8 ng) (Thummel et al., 2006); translation-blocking *kcnh2* MO (5'-CGCGTGGACAGATTCAAGAGCCCTC-3', 2.3 ng)(Arnaout et al., 2007); translation-blocking *tnnt2* MO (5′-CATGTTTGCTCTGATCTGACACGCA-3′, 4 ng) (Sehnert et al., 2002); and 3-OST-5 MO (5'-GTCCAGTCAGGTCAAGGGCAGCTCA-3', 2.7 ng) and 3-OST-3Z MO (5'-GTCCAGTCAGGTCAAGGGCAGCTCA-3', 5.4 ng) as control MOs; Embryos were injected at the 1-2 cell stage.

DAPT treatment

A 25 mM stock of DAPT (Calbiochem) in DMSO was diluted in E3 medium. Embryos were incubated in 75 uM in E3 medium and control embryos were incubated in 0.3% DMSO in E3 medium at 5 hpf, 15 hpf, and 24 hpf. Ventricular contraction was assessed at 48 hpf. Two other incubation periods, one starting at 5 hpf and ending at 24 hpf and the second starting at 15 hpf and ending at 24 hpf, were used. For embryos treated at 5 hpf, somite formation was assessed at 18 hpf to ensure DAPT treatment was

working.

In situ hybridization

Digoxigenin-labeled antisense riboprobes were synthesized using Digoxigenin RNA Labeling Kit (Roche). cDNA plasmids encoding *bmp4*, *versican*, *notch1B* (a gift from Priya Choudhry), *anf*, and *tbx2b* were used. *In situ* hybridizations were performed as previously described (Essner et al., 2000), with anti-digoxigenin antibody incubation carried out using a Biolane HTI machine. Embryos were cleared in 70% glycerol and photographed with a Nikon SMZ1000 camera. Digital images were processed with Adobe Photoshop CS4.

Immunohistochemistry

Immunohistochemistry using the primary antibodies anti-β-catenin (1:200) and anti-DsRed (1:200) was performed as described previously (Neugebauer et al., 2009). Secondary antibodies used were goat anti-mouse Alexa Fluor 488 (Molecular Probes) and donkey anti-rabbit Alexa Fluor 568 (Molecular Probes) in 1:100 dilution. Images were acquired using an Olympus Fluoview FV300 laser scanning confocal microscope. Digital images were processed with Adobe Photoshop CS4.

Rescue in bmp4^{st72} embryos

Embryos from *bmp4*^{st72}/+ x *bmp4*^{st72}/+ matings were injected with 3-OST-7 MO. At 48 hpf, the hearts were scored for noncontracting ventricle, AV defect, or wild-type phenotype. Genomic DNA was extracted from each individual embryo and genotyped using the following dCAPS primers, 5'-TGGTGAGGCACAACACCTCCAACTAG-3' (forward) and 5'-CCGAGTCAGCGGGTGACTTTTGCCGTC-3' (reverse) (generous

gifts from Renee Bend). The PCR products were digested with *SpeI* (NEB) and ran in 3% agarose gel. Digestion with *SpeI* releases 250 bp band in wild-type, 230 bp band in mutant, and both in heterozygotes. DNA genotyped to be from mutants were sequenced to verify compatibility with 3-OST-7 MO.

Cell morphometrics

ImageJ software (NIH) was used to trace cell outlines based on anti-β-catenin staining and to measure the cell surface areas and circularities. Five cells, whose outlines were clearly distinct, were chosen for measurements from each of 10 embryos in each injection group. Circularity was computed by ImageJ using the formula $4\pi A/P^2$. It is a normalized ratio of area (A) to perimeter (P), with a ratio of 1 representing a perfect circle. The circularity values distinguished cells with rounded surfaces from those with elongated surfaces.

Statistics

For comparing cell surface areas and circularity, unpaired t-test was used using GraphPad Prism (version 5.00 for Mac GraphPad Software).

References

Arnaout R, Ferrer T, Huisken J, Spitzer K, Stainier DY, Tristani-Firouzi M, Chi NC (2007) Zebrafish model for human long QT syndrome. Proc Natl Acad Sci U S A 104:11316-11321.

Auman HJ, Coleman H, Riley HE, Olale F, Tsai HJ, Yelon D (2007) Functional modulation of cardiac form through regionally confined cell shape changes. PLoS Biol 5:e53.

Bartman T, Hove J (2005) Mechanics and function in heart morphogenesis. Dev Dyn 233:373-381.

Bartman T, Walsh EC, Wen KK, McKane M, Ren J, Alexander J, Rubenstein PA, Stainier DY (2004) Early myocardial function affects endocardial cushion development in zebrafish. PLoS Biol 2:E129.

Beis D, Bartman T, Jin SW, Scott IC, D'Amico LA, Ober EA, Verkade H, Frantsve J, Field HA, Wehman A, Baier H, Tallafuss A, Bally-Cuif L, Chen JN, Stainier DY, Jungblut B (2005) Genetic and cellular analyses of zebrafish atrioventricular cushion and valve development. Development 132:4193-4204.

Berdougo E, Coleman H, Lee DH, Stainier DY, Yelon D (2003) Mutation of weak atrium/atrial myosin heavy chain disrupts atrial function and influences ventricular morphogenesis in zebrafish. Development 130:6121-6129.

Bulow HE, Hobert O (2006) The molecular diversity of glycosaminoglycans shapes animal development. Annu Rev Cell Dev Biol 22:375-407.

Chi NC, Shaw RM, De Val S, Kang G, Jan LY, Black BL, Stainier DY (2008) Foxn4 directly regulates tbx2b expression and atrioventricular canal formation. Genes Dev 22:734-739.

Esko JD, Lindahl U (2001) Molecular diversity of heparan sulfate. J Clin Invest 108:169-173.

Esko JD, Selleck SB (2002) Order out of chaos: assembly of ligand binding sites in heparan sulfate. Annu Rev Biochem 71:435-471.

Essner JJ, Branford WW, Zhang J, Yost HJ (2000) Mesendoderm and left-right brain, heart and gut development are differentially regulated by pitx2 isoforms. Development 127:1081-1093.

Evans SM, Yelon D, Conlon FL, Kirby ML (2010) Myocardial lineage development. Circ Res 107:1428-1444.

Harvey RP, Meilhac SM, Buckingham ME (2009) Landmarks and lineages in the developing heart. Circ Res 104:1235-1237.

Holley SA, Geisler R, Nusslein-Volhard C (2000) Control of her1 expression during zebrafish somitogenesis by a delta-dependent oscillator and an independent wave-front activity. Genes Dev 14:1678-1690.

Hoogaars WM, Barnett P, Moorman AF, Christoffels VM (2007) T-box factors determine cardiac design. Cell Mol Life Sci 64:646-660.

Huang C, Sheikh F, Hollander M, Cai C, Becker D, Chu PH, Evans S, Chen J (2003) Embryonic atrial function is essential for mouse embryogenesis, cardiac morphogenesis and angiogenesis. Development 130:6111-6119.

Kamimura K, Rhodes JM, Ueda R, McNeely M, Shukla D, Kimata K, Spear PG, Shworak NW, Nakato H (2004) Regulation of Notch signaling by Drosophila heparan sulfate 3-O sulfotransferase. J Cell Biol 166:1069-1079.

Lin X (2004) Functions of heparan sulfate proteoglycans in cell signaling during development. Development 131:6009-6021.

Mably JD, Mohideen MA, Burns CG, Chen JN, Fishman MC (2003) heart of glass regulates the concentric growth of the heart in zebrafish. Curr Biol 13:2138-2147.

Mandel EM, Kaltenbrun E, Callis TE, Zeng XX, Marques SR, Yelon D, Wang DZ, Conlon FL (2010) The BMP pathway acts to directly regulate Tbx20 in the developing heart. Development 137:1919-1929.

Marques SR, Lee Y, Poss KD, Yelon D (2008) Reiterative roles for FGF signaling in the establishment of size and proportion of the zebrafish heart. Dev Biol 321:397-406.

Motoike T, Loughna S, Perens E, Roman BL, Liao W, Chau TC, Richardson CD, Kawate T, Kuno J, Weinstein BM, Stainier DY, Sato TN (2000) Universal GFP reporter for the study of vascular development. Genesis 28:75-81.

Neugebauer JM, Amack JD, Peterson AG, Bisgrove BW, Yost HJ (2009) FGF signalling during embryo development regulates cilia length in diverse epithelia. Nature 458:651-654.

Pellegrini L, Burke DF, von Delft F, Mulloy B, Blundell TL (2000) Crystal structure of fibroblast growth factor receptor ectodomain bound to ligand and heparin. Nature 407:1029-1034.

Reifers F, Walsh EC, Leger S, Stainier DY, Brand M (2000) Induction and differentiation of the zebrafish heart requires fibroblast growth factor 8 (fgf8/acerebellar). Development 127:225-235.

Rottbauer W, Baker K, Wo ZG, Mohideen MA, Cantiello HF, Fishman MC (2001) Growth and function of the embryonic heart depend upon the cardiac-specific L-type calcium channel alpha1 subunit. Dev Cell 1:265-275.

Schlessinger J, Plotnikov AN, Ibrahimi OA, Eliseenkova AV, Yeh BK, Yayon A, Linhardt RJ, Mohammadi M (2000) Crystal structure of a ternary FGF-FGFR-heparin complex reveals a dual role for heparin in FGFR binding and dimerization. Mol Cell 6:743-750.

Scholpp S, Groth C, Lohs C, Lardelli M, Brand M (2004) Zebrafish fgfr1 is a member of the fgf8 synexpression group and is required for fgf8 signalling at the midbrain-hindbrain boundary. Dev Genes Evol 214:285-295.

Sehnert AJ, Huq A, Weinstein BM, Walker C, Fishman M, Stainier DY (2002) Cardiac troponin T is essential in sarcomere assembly and cardiac contractility. Nat Genet 31:106-110.

Shi Y, Katsev S, Cai C, Evans S (2000) BMP signaling is required for heart formation in vertebrates. Dev Biol 224:226-237.

Stainier DY, Lee RK, Fishman MC (1993) Cardiovascular development in the zebrafish. I. Myocardial fate map and heart tube formation. Development 119:31-40.

Stickney HL, Imai Y, Draper B, Moens C, Talbot WS (2007) Zebrafish bmp4 functions during late gastrulation to specify ventroposterior cell fates. Dev Biol 310:71-84.

Thummel R, Bai S, Sarras MP, Jr., Song P, McDermott J, Brewer J, Perry M, Zhang X, Hyde DR, Godwin AR (2006) Inhibition of zebrafish fin regeneration using in vivo electroporation of morpholinos against fgfr1 and msxb. Dev Dyn 235:336-346.

Walsh EC, Stainier DY (2001) UDP-glucose dehydrogenase required for cardiac valve formation in zebrafish. Science 293:1670-1673.

Walters MJ, Wayman GA, Christian JL (2001) Bone morphogenetic protein function is required for terminal differentiation of the heart but not for early expression of cardiac marker genes. Mech Dev 100:263-273.

Westin J, Lardelli M (1997) Three novel Notch genes in zebrafish: implications for vertebrate Notch gene evolution and function. Dev Genes Evol 207:51-63.

Xu X, Meiler SE, Zhong TP, Mohideen M, Crossley DA, Burggren WW, Fishman MC (2002) Cardiomyopathy in zebrafish due to mutation in an alternatively spliced exon of titin. Nat Genet 30:205-209.

Yang L, Cai CL, Lin L, Qyang Y, Chung C, Monteiro RM, Mummery CL, Fishman GI, Cogen A, Evans S (2006) Isl1Cre reveals a common Bmp pathway in heart and limb development. Development 133:1575-1585.

Yayon A, Klagsbrun M, Esko JD, Leder P, Ornitz DM (1991) Cell surface, heparin-like molecules are required for binding of basic fibroblast growth factor to its high affinity receptor. Cell 64:841-848.

CHAPTER 4

DISCUSSION

In this study we have determined the roles of 3-O-sulfotransferase-7 in zebrafish heart development and have uncovered a knockdown model in which to study the relationship between structure and function. 3-OST-7 is required for transcription and accumulation of *tropomyosin4* (*tpm4*) mRNA in the ventricle, ensuring normal levels of Tpm4 and other sarcomeric proteins are present to assemble the sarcomere. Moreover, 3-OST-7 controls a feedback loop between BMP signaling and contraction. In the knockdown model of 3-OST-7, contraction was demonstrated to regulate *bmp4* expression in the ventricle and the transition from isometric to elongated cell shape, both of which are important processes in ventricle maturation.

HSPG modulate processes in cardiac development

The developmental process by which the heart transforms from a bilateral set of precursor cells to the mature, beating organ is orchestrated by a network of growth factors, morphogens, and transcription factor families. Members of this signaling network could act differentially depending upon specific spatiotemporal cues. That heparan sulfate proteoglycans (HSPGs) provide part of these spatiotemporal cues is what I addressed in this dissertation.

The location of HSPGs, on the cell surface or in the extracellular matrix, and their structural heterogeneity place them at a unique advantage to influence signaling pathways

and cell-cell or cell-matrix interactions (Esko and Lindahl, 2001). This versatility has been demonstrated in various animal models where genes coding for the core proteins and proteins involved in biosynthesis and modification of HSPGs have been knocked out or knocked down (Bulow and Hobert, 2006). Notably, two of these genes have been shown to be important at different steps of cardiac formation.

The core protein syndecan 2 (Sdc2) acts in the extraembryonic yolk syncytial layer to direct the bilateral set of heart precursors to fuse (Arrington and Yost, 2009). This is postulated to occur by regulating fibronectin and laminin matrix assembly demonstrating how HSPGs mediate interactions between cells and their environments, interactions that are critical for organogenesis. Meanwhile, UDP glucose dehydrogenase (UGDH), an enzyme involved in the synthesis of heparan sulfate, chondroitin sulfate and hyaluronic acid, is required for cardiac valve formation in zebrafish (Seidman and Seidman, 2001; Walsh and Stainier, 2001). Interestingly, Sugarless, the *Drosophila* homolog of UGDH, has been shown to be important in the FGF and Wnt signaling pathways (Binari et al., 1997; Hacker et al., 1997; Haerry et al., 1997; Lin et al., 1999). This illustrates an essential role HSPGs play in transducing signals from extracellular ligands into the cell.

The ability of HSPGs to modulate these processes are partly due to the glycosaminoglycan chains attached to the core proteins and their associated modifications (Esko and Selleck, 2002). In this dissertation I examined the functions of 3-OST-7 in zebrafish heart development. 3-OST-7 is a member of the zebrafish 3-OST family, whose expression patterns suggest distinct roles in the developing embryo (Cadwallader and Yost, 2006). Knockdown of 3-OST-7 resulted in a noncontracting ventricle where

contraction has been uncoupled from excitation because of sarcomere defects. Additionally, knockdown of 3-OST-7 uncovered a feedback loop between *bmp4* expression and contraction, making this a favorable model for studying the relationship between structure and function.

3-OST-7 controls ventricular contraction

Contraction of the heart is downstream of excitation events that transduce the electrical stimulus from the sinus venosus to the atrium and then to the ventricle. Cardiac excitation events, specifically the generation of action potentials and calcium transients, were demonstrated to be normal in 3-OST-7 morphant atrium and ventricle. In contrast, ventricular contraction was defective. The spatiotemporal specificity of this phenotype highlights the level of specificity of 3-OST-7-dependent 3-O-sulfation. The ubiquitous expression of 3-OST-7 (Cadwallader and Yost, 2006) suggests it functions in all tissues. However, it appears dispensable in other tissues but is strictly required in the ventricle, since knockdown of 3-OST-7 resulted in a ventricle-specific defect. Moreover, rescue of the noncontracting ventricle in transgenic *Tg(β-actin:3-OST-7-IRES-EGFP)* embryo, which ubiquitously overexpresses 3-OST-7, and not in *Tg(cmlc2:3-OST-7-IRES-EGFP)*, which overexpresses 3-OST-7 only in the myocardium, suggests 3-OST-7 is required in a neighboring, non-*cmlc2* expressing tissue. Another possibility is that the timing of the *cmlc2*-driven transgene is off, which still underscores the importance of temporal specificity for 3-OST-7 activity in ventricular contraction. It would be interesting to see whether the use of other cardiac-specific drivers that will overexpress 3-OST-7 in other cardiac tissues such as the endocardium and the epicardium will rescue ventricular

noncontraction. This will elucidate the intricacy of interactions among cardiac tissues required for normal cardiac function and development.

3-OST-7 controls myofibrillogenesis

For normal heart contraction to occur, contractile proteins must be produced and assembled in units called sarcomeres. This process termed myofibrillogenesis gives rise to a thick filament system, composed mostly of myosin, and a thin filament system, consisting of actin, troponin, and tropomyosin. The highly organized sarcomere ensures coordinated generation of force from regulated interaction of actin and myosin filaments. Knockdown of 3-OST-7 interferes with the process of myofibrillogenesis as assessed by appearance of aberrant sarcomeric proteins from immunohistochemical staining of actin, cardiac troponin T (Tnnt2), and Tpm. Our findings support the concept that loss of a sarcomere protein impacts on the stability of other sarcomere proteins and the sarcomere as a whole, because strikingly, only *tpm4* transcripts were reduced in 3-OST-7 morphants. More importantly, overexpression of Tpm4 protein by injection of *tpm4* RNA, rescued the noncontracting ventricle. This suggests Tpm4 acts as a lynchpin protein and that normal levels of Tpm4 stabilize Tnnt2 and possibly another tropomyosin protein, Tpma (Zhao et al., 2008). Moreover, the resulting reduction of Tnnt2 could likewise affect Tpm and other sarcomere proteins such as TnI (Sehnert et al., 2002). These indicate the existence of a feedback mechanism to ensure proteins within a sarcomere are stabilized in a coordinated manner.

Our findings also demonstrate that ventricular contraction does not occur normally in 3-OST-7 morphants because contraction is uncoupled from excitation,

placing 3-OST-7 dependent 3-O-sulfation in a novel pathway that regulates myofibrillogenesis.

3-OST-7 controls morphogenesis

Transitioning from an isometric to an elongated morphology is one of the hallmarks of ventricular myocyte maturation (Auman et al., 2007). Knockdown of 3-OST-7 perturbed this morphogenetic process, resulting in isometric ventricular cardiomyocytes that differ from ventricular myocytes found in normal embryos of the same stage. The defect in morphogenesis is not due to an overall defect in maturation because markers for the chamber (working) myocardium, nonchamber (nonworking) myocardium, and the endocardium were normally expressed.

The relationship between structure and function is a popular theme in heart development (Bartman et al., 2004; Bartman and Hove, 2005; Auman et al., 2007). Because the heart starts to beat even before it completes its formation, possibly affecting subsequent processes of differentiation, the observed failure of ventricular cardiomyocytes to elongate could be a result of ventricular noncontraction. Since we have shown *tpm4* is downstream of 3-OST-7 in regulating contraction, it would be interesting to see whether *tpm4* mutants and morphants possess the same isometric ventricular cardiomyocytes as 3-OST-7 morphants. Interestingly, the isometric cardiomyocyte morphology observed in 3-OST-7 morphants was not observed in two distinct contraction defect models, *kcnh2* and *tnnt2* morphants, however ventricular cardiomyocytes in these two morphants had subtle differences from control cardiomyocytes. This suggests that the relationship between structure and function is complex and is dependent on the pathway that perturbs contraction. It also supports

previous studies where the use of zebrafish mutants have demonstrated that contractility and blood flow have contrasting effects on cardiomyocyte dimensions (Auman et al., 2007).

3-OST-7 controls a feedback loop between *bmp4* signaling and contraction

Restriction of genes to specific regions of the heart is part of the sub-specialization process the heart undergoes during its maturation (Evans et al., 2010). Knockdown of 3-OST-7 resulted in ectopic expression of *bmp4* and versican in the ventricle. This ectopic expression appeared to be due to ventricular noncontraction because noncontraction and ectopic *bmp4* expression were correlated in *kcnh2* and *tnnt2* morphants as well. Strikingly, ventricular noncontraction in 3-OST-7 morphants was rescued by the $bmp4^{st72}$ mutation. This suggests a feedback loop exists between *bmp4* signaling and contraction and that this feedback loop is controlled by 3-OST-7. I anticipate that defining the pathways that mediate this feedback loop will greatly improve our understanding of cardiac morphogenesis and will continue to highlight the significance of 3-OST-7 dependent 3-O-sulfation in cardiac development, physiology and function.

Role of signaling pathways in transducing 3-OST-7 signal

Experiments that sought to perturb the FGF and Notch signaling pathways have demonstrated that these pathways are not likely transducing the 3-OST-7 signal. However, it is likely that these pathways act in concert to regulate ventricular contraction and a more global strategy is required to tease apart these interactions. In line with this, we performed microarray analysis to determine the differences in transcription profiles

between wild-type and 3-OST-7 morphant hearts and to possibly identify signaling pathways that we have not looked at previously. Using *t*-test to identify statistically significant profiles, 727 genes were shown to be down-regulated and 1823 were up-regulated. The most dramatically regulated genes were not known members of major developmental signaling pathways. Future gene ontology analysis or analysis based on grouping genes by their functions might improve identification of relevant genes.

Role of core proteins in cardiac development

This dissertation has primarily focused on 3-OST-7 dependent modification of GAG chains, but an important aspect of modulation by HSPGs is through their core proteins (Esko and Selleck, 2002). Knockdown of Sdc2 has demonstrated a core protein could act in a specific step of cardiac formation (Arrington and Yost, 2009). It would be interesting to know which core proteins, when mutated or knocked down, give a similar phenotype as knockdown of 3-OST-7. Although knockdown of Sdc2 does not give a cardiac phenotype similar to knockdown of 3-OST-7 (unpublished data, personal communications with C.B. Arrington), there are three more syndecans and 10 glypicans that could be acting independently or in concert to ensure normal cardiac function.

Role of other 3-OSTs in cardiac development

3-OST-7 is one of eight 3-OSTs in zebrafish, making it possible there are other 3-OSTs involved in heart development. We have explored this possibility by knocking down several other members of the 3-OST family, and found that only one other member, 3-OST-1, the closest relative of 3-OST-7, has a similar cardiac phenotype as knockdown of 3-OST-7. Both knockdowns resulted in similar penetrance of ventricular noncontraction. Furthermore, double knockdown of 3-OST-7 and 3-OST-1 increased

penetrance of the cardiac ventricular phenotype, arguing that these two 3-OSTs are partially functionally redundant. It would be interesting to see whether ventricular noncontraction in 3-OST-7 morphants could be rescued by overexpression of 3-OST-1 RNA. Of interest too is whether these two 3-OSTs modulate the same pathways to affect ventricular contraction. Interestingly, knockdown of 3-OST-1 has a more severe effect on the heart, including defects in atrial contraction, suggesting 3-OST-1 regulates other aspects of cardiac formation. Further exploration of the cardiac phenotype in 3-OST-1 morphants will help elucidate the unique roles of 3-OST-1.

Conclusion

I have demonstrated in this dissertation that 3-OST-7 regulates novel processes of cardiac development. 3-OST-7 controls ventricular contraction by controlling myofibrillogenesis and mediates structure-function relationships by controlling *bmp4* expression. Further exploration of the 3-OST-7 knockdown model could uncover signaling mechanisms and transducers that regulate cardiac development and physiology.

References

Arrington CB, Yost HJ (2009) Extra-embryonic syndecan 2 regulates organ primordia migration and fibrillogenesis throughout the zebrafish embryo. Development 136:3143-3152.

Auman HJ, Coleman H, Riley HE, Olale F, Tsai HJ, Yelon D (2007) Functional modulation of cardiac form through regionally confined cell shape changes. PLoS Biol 5:e53.

Bartman T, Hove J (2005) Mechanics and function in heart morphogenesis. Dev Dyn 233:373-381.

Bartman T, Walsh EC, Wen KK, McKane M, Ren J, Alexander J, Rubenstein PA, Stainier DY (2004) Early myocardial function affects endocardial cushion development in zebrafish. PLoS Biol 2:E129.

Binari RC, Staveley BE, Johnson WA, Godavarti R, Sasisekharan R, Manoukian AS (1997) Genetic evidence that heparin-like glycosaminoglycans are involved in wingless signaling. Development 124:2623-2632.

Bulow HE, Hobert O (2006) The molecular diversity of glycosaminoglycans shapes animal development. Annu Rev Cell Dev Biol 22:375-407.

Cadwallader AB, Yost HJ (2006) Combinatorial expression patterns of heparan sulfate sulfotransferases in zebrafish: I. The 3-O-sulfotransferase family. Dev Dyn 235:3423-3431.

Esko JD, Lindahl U (2001) Molecular diversity of heparan sulfate. J Clin Invest 108:169-173.

Esko JD, Selleck SB (2002) Order out of chaos: assembly of ligand binding sites in heparan sulfate. Annu Rev Biochem 71:435-471.

Evans SM, Yelon D, Conlon FL, Kirby ML (2010) Myocardial lineage development. Circ Res 107:1428-1444.

Hacker U, Lin X, Perrimon N (1997) The Drosophila sugarless gene modulates Wingless signaling and encodes an enzyme involved in polysaccharide biosynthesis. Development 124:3565-3573.

Haerry TE, Heslip TR, Marsh JL, O'Connor MB (1997) Defects in glucuronate biosynthesis disrupt Wingless signaling in Drosophila. Development 124:3055-3064.

Lin X, Buff EM, Perrimon N, Michelson AM (1999) Heparan sulfate proteoglycans are essential for FGF receptor signaling during Drosophila embryonic development. Development 126:3715-3723.

Sehnert AJ, Huq A, Weinstein BM, Walker C, Fishman M, Stainier DY (2002) Cardiac troponin T is essential in sarcomere assembly and cardiac contractility. Nat Genet 31:106-110.

Seidman JG, Seidman C (2001) The genetic basis for cardiomyopathy: from mutation identification to mechanistic paradigms. Cell 104:557-567.

Walsh EC, Stainier DY (2001) UDP-glucose dehydrogenase required for cardiac valve formation in zebrafish. Science 293:1670-1673.

Zhao L, Zhao X, Tian T, Lu Q, Skrbo-Larssen N, Wu D, Kuang Z, Zheng X, Han Y, Yang S, Zhang C, Meng A (2008) Heart-specific isoform of tropomyosin4 is essential for heartbeat in zebrafish embryos. Cardiovasc Res 80:200-208.